Journal of Plant Physiology
Manuscript Draft

Manuscript Number: JPLPH-D-16-00735

Title: UV-vis spectroscopy and colorimetric models for detecting anthocyanin-metal complexes in plants: an overview of in vitro and in vivo techniques

Article Type: Review Article

Section/Category: Physiology

Keywords: Anthocyanins-metal complexes; Color measurement; Copigmentation; Difference reflectance spectroscopy; Derivative spectroscopy; UV-vis spectroscopy.

Abstract: Although anthocyanin (ACN) biosynthesis is one of the best studied pathway of secondary metabolism in plants, the possible physiological and ecological role(s) of these pigments continue to intrigue scientists. Like other dihydroxy B-ring substituted flavonoids, ACNs have an ability to bind metal and metalloid ions, a property that has been exploited for a variety of purposes. For example, the metal binding ability may be used to stabilize ACNs from plant food sources, or to modify their colors for using them as food colorants. The complexation of metals with cyanidin derivatives can also be used as a simple, sensitive, cheap, and rapid method for determination concentrations of several metals in biological and environmental samples using UV-vis spectroscopy. Far less information is available on the ecological significance of ACN-metal complexes in plant-environment interactions. Metalloanthocyanins (protocyanin, nemophilin, commelinin, protodelphin, cyanosalvianin) are involved in the copigmentation phenomenon that leads to blue-pigmented petals, which may facilitate specific plant-pollinator interactions. ACN-metal formation and compartmentation into the vacuole has also been proposed to be part of an orchestrated detoxification mechanism in plants which experience metal/metalloid excess. However, investigations into ACN-metal interactions in plant biology may be limited because of the complexity of the analytical techniques required. To address this concern, here we describe simple methods for the detection of ACN-metal both in vitro and in vivo using UV-vis spectroscopy and colorimetric models. In particular, the use of UV-vis spectra, difference absorption spectra, and colorimetry techniques will be described for in vitro determination of ACN-metal features, whereas reflectance spectroscopy and colorimetric parameters related to CIE L*a*b* and CIE XYZ systems will be detailed for in vivo analyses. In this way, we hope to make this high-informative tool more accessible to plant physiologists and ecologists.

UV-vis spectroscopy and colorimetric models for detecting anthocyanin-metal complexes in plants: an overview of *in vitro* and *in vivo* techniques

Volodymyr S. Fedenko[1], Sergiy A. Shemet[1], Marco Landi[2*]

[1]*Scientific Research Institute of Biology, Oles Honchar Dnipropetrovsk National University, 72 Gagarin Avenue, Dnipro, Ukraine, 49010*

[2]*Department of Agriculture, Food and Environment, University of Pisa, Via del Borghetto, 80 I-56124, Pisa, Italy*

*Corresponding author:
Dr. Marco Landi
Department of Agriculture, Food & Environment, University of Pisa
Via del Borghetto, 80; I-56124, Pisa, Italy
Tel: +39 050 2216620
E-mail address: marco.landi@for.unipi.it (M. Landi)

ABSTRACT

Although anthocyanin (ACN) biosynthesis is one of the best studied pathway of secondary metabolism in plants, the possible physiological and ecological role(s) of these pigments continue to intrigue scientists. Like other dihydroxy B-ring substituted flavonoids, ACNs have an ability to bind metal and metalloid ions, a property that has been exploited for a variety of purposes. For example, the metal binding ability may be used to stabilize ACNs from plant food sources, or to modify their colors for using them as food colorants. The complexation of metals with cyanidin derivatives can also be used as a simple, sensitive, cheap, and rapid method for determination concentrations of several metals in biological and environmental samples using UV-vis spectroscopy. Far less information is available on the ecological significance of ACN-metal complexes in plant-environment interactions. Metalloanthocyanins (protocyanin, nemophilin, commelinin, protodelphin, cyanosalvianin) are involved in the copigmentation phenomenon that leads to blue-pigmented petals, which may facilitate specific plant-pollinator interactions. ACN-metal formation and compartmentation into the vacuole has also been proposed to be part of an orchestrated detoxification mechanism in plants which experience metal/metalloid excess. However, investigations into ACN-metal interactions in plant biology may be limited because of the complexity of the analytical techniques required. To address this concern, here we describe simple methods for the detection of ACN-metal both *in vitro* and *in vivo* using UV-vis spectroscopy and

colorimetric models. In particular, the use of UV-vis spectra, difference absorption spectra, and colorimetry techniques will be described for *in vitro* determination of ACN-metal features, whereas reflectance spectroscopy and colorimetric parameters related to *CIE* $L^*a^*b^*$ and *CIE XYZ* systems will be detailed for *in vivo* analyses. In this way, we hope to make this high-informative tool more accessible to plant physiologists and ecologists.

Keywords: Anthocyanins-metal complexes; Color measurement; Copigmentation; Difference reflectance spectroscopy; Derivative spectroscopy; UV-vis spectroscopy

Abbreviations: ΔA_{max}, variation of maximal absorbance intensity; $\Delta\lambda_{max}^{uv}$, difference of maximal absorbance wavelength in UV region; $\Delta\lambda_{max}^{vis}$, difference of maximal absorbance wavelength in visible region; λ_d, dominating wavelength; λ_{max}, maximal absorbance wavelength; λ_{min}, minimal absorbance wavelength λ'_{max}, first derivative of maximal absorbance wavelength; A_{max}, maximal absorbance intensity; A'_{max}, first derivative of maximal absorbance intensity; ACNs, anthocyanins; ACN-Me^{n+}, anthocyanin-metal complexes; Cy, cyanidin; Cy-3-glu, cyanidin-3-glucoside; Dp, delphinidin; DRA, dorsal rim area; FC, form coefficient; GSH, glutathione; Me^{n+}, metal ions; Mv, malvidin; P_e, excitation purity; Pg, pelargonidin; Pn, peonidin; Pt, petunidin.

Contents

1. Introduction

Anthocyanin (ACN) pigments are colorful flavonoids (ranging from light pink to dark blue) which are responsible for the marvelous color versatility of plant kingdom (Grotewold, 2006). As other polyphenols, ACNs play some key ecological roles as they are involved in multiple plant-environment interactions, realization of reproductive strategy and defense mechanisms (Cheynier et al., 2013; Gould et al., 2009; Gould 2010), even though the main ecological function (if any) which has driven the evolution of these pigments in angiosperm groups is still highly debated (Archetti et al., 2009; Hughes, 2011; Landi et al., 2015; Manetas, 2006; Menzies et al., 2016; Ougham et al., 2008).

ACNs are di- or tri-hydroxy B-ring-substituted flavonoids containing a flavylium cation (Fig. 1) which, owing to its conjugated double bonds, absorbs visible light with a peak in the 500-550 nm wavebands. ~~In view of~~ ACN instability at neutral to weakly acid pH ~~due~~ to the hydration of flavylium cation ~~to~~ the colorless pseudobase, complexation of these pigments has been shown to contribute to the increased stability of ACNs in solution (Ellestad, 2006; Yoshida et al., 2009). Copigmentation is a natural phenomenon which occurs when ACNs interact with other compounds such as phenolic acids, flavonoids (including other ACNs), and/or metal ions (Me^{n+}) to self-assemble in supramolecular complexes. The resulting complexes prevent the labile flavylium cation from nucleophile attack and can protect ACNs from degradation due to high pH and temperature (Zhang et al., 2009). ~~As similar as~~ to other colorless flavonoids, the ability of ACNs to create complexes with Me^{n+} is primarily determined by their chemical structure as glycosylated hydroxy- and methoxy-derivates of 2-phenylbenzopyrylium (flavylium) salt (Fossen and Andersen, 2006). Noteworthy, ~~that~~ huge variety of ACNs found in plant kingdom (to date more than 600 different anthocyanins have been isolated) (Guidi et al., 2015) is created by only six aglycones (Andersen and Jordheim, 2006). ~~Bearing in mind~~ the Me^{n+}-binding ability of ACNs, those compounds should be divided into two groups. The first group comprises ACNs with two or three hydroxyl substitutes in the B ring: cyanidin- (Cy), delphinidin- (Dp), petunidin- (Pt)-derivatives (Fig. 2). These compounds usually bind to Me^{n+} by two -OH substitutes in *ortho*-position in the B ring (catechol or pyrogallol moiety). The second group comprises ACNs with a single hydroxyl substitute (pelargonidin; Pg-derivatives) and with one (peonidin; Pn-derivatives), or two methoxyl substitutes in the B ring (malvidin; Mv-derivatives) (Fig. 2). For this latter group, the Me^{n+} chelation mechanism is far less probable, even though complexes with Au nanoparticles (with the participation of a single hydroxyl group) were recently described (Zaffino et al., 2015).

Critically important feature of ACNs consists in the pH-dependent dynamic equilibrium of their different structural forms in ~~water~~ solutions which distinguishes them from other flavonoids and favors their binding with Me^{n+}. The schematic diagram of those structural transformations is shown

in Fig. 3 (rearranged from Buchweitz, 2016; Pina et al., 2012; Trouilas et al., 2016) with Cy-3-glucoside (Cy-3-glu) as an example. Flavylium ion (AH^+) predominates at pH < 2 and show red color, whereas increases of pH drive series of reversible (to some extent) chemical transformations. At pH > 2 the hydration of flavylium cation leads to the prevalent formation ~~of~~ a colorless hemiketal form (B), which transforms tautomerically ~~into~~ a yellow *cis*-chalcone and isomerizes to *trans*-chalcone. Proton transfer turns red flavylium ion (AH^+) into neutral quinoidal base, some forms of which have purple color tonalities. At pH 6-8, blue forms of anionic quinoidal base (A^-) are predominant. Binding to Me^{n+} shifts the equilibrium between different structures toward the creation of blue quinoidal form and tend to stabilize the resulting structure.

Among all the flavonoids, the metal-binding ability of ACN is of greatest interest for the following reasons. Firstly, the ACN-Me^{n+} binding ability is exploited to stabilize ACN from edible sources and to modify their colors for using them as food colorants (Buchweitz et al., 2013a, 2013b; Sigurson, Giusti, 2014). Secondly, metal complexation with Cy-based compounds has been used as a simple, sensitive, cheap, rapid and environmental friendly multi-element metal determination using UV-vis spectroscopy (Okoye et al., 2012; 2013). In addition to the exploitation of this feature for human purposes, from an ecological point of view this ability of ACNs is one of the main determinants underlying the copigmentation phenomenon, which stabilizes and modifies flower color of many plant species (Ellestad, 2006; Trouillas et al., 2016; Yoshida et al., 2009). Resulting blue, violet and purple colors broadens the diversity of plant coloration as the basis of their interaction with pollinators (Foster et al., 2014; Yoshida et al., 2009). Furthermore, ACNs complexation with different Me^{n+} and compartmentation of ACN-Me^{n+} complexes (ACN-Me^{n+}) into the vacuole is believed to be one of the detoxification mechanisms in plants which experience metal excess (Hale et al., 2001, 2002, Fedenko, 2006a, 2008, Landi, 2015; Landi et al., 2015).

Unlike sophisticated methods routinely utilized by chemists for detecting ACN-Me^{n+} (i.e. in food science, environmental science, chemistry of textile dying), relatively simple, affordable, informative and cheap methods should be suggested to describe ACN-Me^{n+} formation, especially for plant ecologists and plant biologist who are principally interested (at least at a first approach) in the occurrence of those complexes rather than to their intimal chemical structure. The actual complexity of the investigation of ACN-Me^{n+} interaction is due to the variety of analytical techniques used to study different aspects of the metal-binding ability of ACN. To date, UV-vis spectroscopy, Raman, Nuclear Magnetic Resonance, and Circular Dichroism spectroscopy are the most widely utilized techniques (Buchweitz et al., 2013a; Trouillas et al., 2016) and among them, conventional UV-vis spectroscopy is considered to be the one of most informative analytical tools (Trouillas et al., 2016). UV-vis spectroscopy is based on the principle for which the binding of ACNs to Me^{n+} changes the conjugation of the chromophore system of ACNs, which is, in turn,

accompanied by chromatic changes. Thus, the registration of spectral characteristics in visible wavebands as well as additional absorption maximum in the UV region is the most feasible way to confirm such changes (Jangantakumar and Shukla, 2014; Okoye et al., 2013).

It is worthy to note that the majority of the studies concerning ACN-Me^{n+} interaction were done *in vitro* using pigment extracts, individual natural compounds, or their synthetic analogues. However, to determine the role/effect of metal-binding ability of ACNs on plant physiology, analytical tools for the *in vivo* detection of this effect (when possible) should be preferred. During the implementation of such techniques, several considerations should be taken into account as follows: Firstly, one of the characteristic features of ACNs is their main localization in outer layers of plant tissues (despite in some cases ACNs can reside in inner tissues; i.e. vacuole of mesophyll cells). This implies the use of non-destructive analytical methods as extraction of ACN-Me^{n+} from plant specimens can lead to the disruption of these associations. Secondly, ACNs are capable to interact simultaneously with different Me^{n+} in solution (Toyama-Kato et al., 2003), thus the *in vitro* metal stoichiometry of ACN-Me^{n+} (associated *versus* unassociated form) may differ from the stoichiometric ratios determined *in vivo*. Thirdly, as the binding process can occur not simultaneously for all ACN molecules in intact plants (because of time-dependent Me^{n+} accumulation in plant tissue), the evaluation of ACN-Me^{n+} in extracted pigments can lead to misleading results concerning the coexistence of different ratios between associated (bonded) and unassociated (unbounded) ACNs.

Taking into consideration the aforementioned issues concerning the *in vivo* identification of ACN-Me^{n+} interactions, the simultaneous implementation of different spectrophotometric methods should be preferred (Fedenko et al., 2005; Fedenko and Struzhko, 2000). This means that different analytical techniques are not to be used separately but connected in a unified, affordable and highly-informative methodology. This methodology is based on the interaction of optical radiation with ACN molecules, both as associated and unassociated form, and on the use of various spectrophotometric parameters having different informational value.

In view of the steady increase of interest toward the interaction between ACN and Me^{n+} in plants and the growing number of related publications, there is the need of a critical overview of spectrophotometric criteria for the detection of the ACN-Me^{n+} binding, both *in vitro* and *in vivo*. In addition, there is the necessity to simplify the description of UV-vis spectroscopy methodologies to make those analyses more accessible to a wide range of plant biologists with the attempt to stimulate further researches. The present review describes some methodologies applied for spectrophotometric and colorimetric detection of ACN-Me^{n+} either in solution and in intact plant tissue. In case of optical radiation transmitted through an ACN-containing solution, the pigment selectively absorbs part of the light stream and transmits the remaining part, thus the criteria for the

determination of ACN-Me^{n+} binding in solution could be the observation of changes in the absorption and colorimetric parameters (Fedenko et al., 2005; Sigurson and Giusti, 2014). In other cases, when optical radiation interacts with ACNs associated with Me^{n+} in plant tissues, part of the optical radiation is selectively absorbed *in vivo* and another part of the radiation is reflected, the effect determining the color stimuli of pigmented specimen. For the latter case, parameters derived from non-destructive methods of reflectance spectroscopy and tristimulus colorimetry can be used (Fedenko and Struzhko, 2000).

2. Ecological role of anthocyanin-metal complexes in plants

The first experiments that demonstrated the metal-chelating ability of ACNs were conducted in the late 1910s by Shibata and co-workers (Shibata et al., 1919) who posed the base for the theory of the blue color development of *Centaurea cyanus* flowers. That theory becomes realistic only several years later when Hayashi (1957) and Hayashi et al. (1958) isolated a blue pigment flowers of *Commelina communis* (they named the pigment "commelinin") and demonstrated that commelinin is complex metal-coordinated pigment which consist of ACNs, flavones and Mg^{2+} ions. However, only many years later Kondo et al. (1992) determined the full structure of commelin by X-ray crystallography and had described with the term 'metalloanthocyanin' a self-assembled, supramolecular, noncovalent, metal complex pigment composed of stoichiometric amounts of ACNs, flavones, and Me^{n+} (6:6:2, respectively). The presence of Me^{n+} as well as the strong concentration of these supramolecular complexes in vacuoles (mM range; Ellestad, 2006) is essential for complex formation and to the stability of metalloanthocyanins whose color disappear, indeed, in weak solutions (Takeda and Hayashi, 1977). This is due to the weak interactions that occur in metalloanthocyanins, such as metal complexation and hydrophobic interactions between the chromophores of ACNs and flavones. The blue color is generated by Me^{n+} complexation with the quinonoidal base (anion form) of the anthocyanidin chromophore, and this form is stabilized by self-association and copigmentation (Yoshida et al., 2015). The complexation is necessary for a stable blue color development of flower petals given that the weakly acid vacuolar pH (where ACNs accumulate) would induce the vacuolar solution to be purple-red rather than blue. After the characterization of commelinin, other metalloanthocyanins have been identified: protocyanin from *C. cyanus* (Bauer, 1958; Shiono et al., 2005), cyanosalvianin from *Salvia uliginosa* (Mori et al., 2008), protodelphin from *Salvia patents* (Kondo et al., 2001; Takeda et al., 1994), nemophilin from *Nemophila menziesii* (Yoshida et al., 2015). ACN-Me^{n+} have not only been found as supramolecules, but also as non-stoichiometric metal complexes in petals, such as those found in blue flowers of *Hydrangea macrophylla* (Kondo et al., 1994; Takeda 1985) and *Tulipa gesneriana* (Shoji et al., 2007).

It is likely that some plant species have evolved blue petals to attract selectively insect pollinators, some of which are only equipped with three types of photoreceptors, maximally sensitive to green, blue, and UV light (Kirchner et al., 2005). Differently, many red-coloured and red-flowered plant species are usually pollinated by birds, which have a red receptor (Rodríguez-Gironés and Santamaria, 2004), or even by insect pollinators that are more attracted, for example, by plant volatiles than by visual cues. For those insects which preferentially use UV rather than visible waveband to locate plants and plant organs, the increased UV absorbance of plant tissues which occurs when ACNs conjugate to Me^{n+} can increase the conspicuousness of flowers by increasing the contrast between UV-absorbing flower patches (rich in ACN-Me^{n+}) and surrounding areas which does not absorb UV wavebands, such as UV-reflecting areas rich in carotenoids (Fedenko and Struzhko, 2000; Miller et al., 2011). One of the best documented examples of this mechanism is the 'honey guide' of *N. meziesii* flowers, whose petals are blue at their distal region (due to the presence of nemophilin, Yoshida et al., 2015) whereas they are carotenoid-rich in the yellow proximal regions. The achromatic contrast (black *vs* UV-reflecting areas) drives 'wisely' bees to the nectar; conversely, the chromatic contrast (blue *vs* yellow flower patches), as perceivable for example by the UV-insensitive human eyes, would be far less efficient to locate the flower in the context of surrounding vegetation.

In addition to diffuse light, sunlight reflecting off shiny surfaces (such as water surface and leaves) is also linearly polarized (Wehner, 2001) and can serve as a key navigational cue being perceived by many animals, including insects. Polarization-sensitive ommatidia exist in the dorsal periphery of many insect retinas, forming the so called dorsal rim area (DRA; Wernet et al., 2012), or throughout their eye (Kelber et al., 2001), in addition to the DRA. Despite it has been thought for many years that the only function of polarization vision in insects was restricted to sun-compass navigation, other intriguing additional functions have been recently proposed and, to the best of our knowledge, these include the first evidence that bees may use polarization vision to learn polarization patterns on flowers (Foster et al., 2014). In particular, Foster et al. (2014) demonstrated that foraging bumblebees can learn to discriminate between two differently-polarized artificial flowers and this feature seems related to the ability of their retina and ocelli to perceive blue- and UV-polarized light (Ribi et al., 2011), both the wavebands absorbed by ACN-Me^{n+} complexes.

It is clear that plant and insect fitness are strictly interdependent and both correlated to the capacity of pollinators to accurately discriminate flowers (and flower organs) *via* different cues, including UV and/or vis light emission. Given ~~that~~ different Me^{n+} can be artificially replaced in metalloanthocyanins (Nigel and Grayer, 2008; Yoshida et al., 2015) and that those replacements would alter their UV-vis absorbance (reviewed by Yoshida et al., 2009), it is likely that plants growing in metal-rich soils accumulate different types (and/or different proportions) of Me^{n+}, thus

leading their flower to have a different UV-vis spectrum. So that, it would be really interesting to compare the behaviour of pollinators when plants experience such conditions of metal toxicity to understand the ecological effect of changes in ACN-Me^{n+} composition in terms of number of flower's visits and reproductive success of the plant species.

Another important aspect which involves the formation of ACN-Me^{n+} complexes in plants is the condition of metal- and metalloid-induced toxicity. Accumulation of ACNs in roots and aboveground plant organs is believed to be one of the predominant tendency in response to metal/metalloid toxic levels, both in soils and nutrient solutions: Cd (Dai et al., 2012; Růžičková et al., 2015; Shemet and Fedenko, 2005), Zn (Asad et al., 2015; Kösesakal and Ünal, 2012; Park et al., 2012), Pb (Růžičková et al., 2015), Mo (Baldisseroto et al., 2010; Hale et al., 2001), W (Hale et al., 2002). U (Doustaly et al., 2014), Se (Hawrylak-Nowak, 2008), As (Leão et al., 2014; Růžičková et al., 2015), B (Cervilla et al., 2012; Eraslan et al., 2016; Landi at al., 2014; Pardossi et al., 2015). Under these circumstances, it has been proposed that accumulation of ACNs, and in particular of ACN-Me^{n+}, might be part of a detoxifying mechanism which would confer a higher degree of metal/metalloid tolerance to plants (Baldisseroto et al., 2010; Landi 2015; Landi et al., 2015; Růžičková et al., 2015). However, only few studies have demonstrated the metal-chelating ability of ACNs in intact plants (Fedenko, 2006a, 2007, 2008; Hale et al., 2001, 2002; Shemet and Fedenko, 2005).

In view of (i) the strict interdependence between metal and ACNs in plants which experience metal-toxicity; (ii) the evidence that pigmented plants utilized for phytoremediation usually have higher fitness than acyanic morphs (Chalker-Scott, 1999; Hale et al., 2001; Pilon-Smits and Pilon, 2002); (iii) the metabolic cost associated with the biosynthesis of ACNs, a high metabolic effort sustained by plants, especially in condition of metal-induced physiological and biochemical alterations, it seems logical to suppose that ACNs biosynthesis is not only a side effect induced by metal toxicity, but rather a key response of plants in condition of metal excess. However, the answer to the question: "What is the ecological role of these latter non-stoichiometric ACN-Me^{n+} in plants?" is far from being obvious. One of the most convincing hypothesis is that the formation of ACN-Me^{n+} in plant tissue may alleviate the metal-induced toxicity by sequestration of supernumerary Me^{n+} in peripheral cell layers, apoplastic space and/or cell vacuole where they are less harmful than in cytosol and photosynthetic mesophyll. In addition, ACN-Me^{n+} can effectively increase absorption of UV-vis wavelengths, as reported for ACN-Me^{n+} which involve Al (Schreiber et al., 2010), Mg (Kondo et al., 1992), Fe (Everest and Hall, 1921), Mo (Hale et al., 2001), W (Hale et al., 2002), thereby offering an additional defence against excess of light, especially when chloroplast functioning is already impaired by metal toxicity. The increased UV absorption of plant tissues due to ACN-Me^{n+} formation can be particularly advantageous to avoid chronic

photoinhibition of PSII, in particular to contrast damages related to the protein D1 and the oxygen evolving complex, two of the most sensible sites to high UV irradiance (Takahashi and Badger, 2011). In addition, given that both ACNs and Me^{n+} (the latter principally when in excess) share similar vacuolar transporters (i.e. glutathione; GSH, and GSH S-transferases) this raises the possibility of a cross-talk between these carriers and the probability that formation of ACN-Me^{n+} might expedite the vacuolar accumulation of supernumerary Me^{n+} (Landi et al., 2015). The latter authors also suggested that the mechanism involving ACNs transiently bind to Me^{n+} in the cytosol would be also energetically efficient in terms of GSH cell balance to shuttle those compounds into the vacuole; instead of requiring one molecule of GSH to complex with a molecule of ACN and another GSH molecule (or even two) to sequestrate a Me^{n+}, the proposed mechanism would require only a single molecule of GSH to transport an ACN moieties conjugated with a Me^{n+}. In this way, part of GSH pool could be devoted to other roles, such as to regenerate oxidized ascorbic acid that usually has a key role as low molecular weight antioxidant against the metal-triggered free radical production.

Recently, the same ability of foliar ACNs has also been postulated for B that, differently to the elements previously mentioned, is a metalloid (Landi, 2015; Landi et al., 2014; 2015; Pardossi et al., 2015). This ability was previously reported for other *cis*-diols, including other phenols *sensu lato* (Brown et al., 2002), including luteolin and quercetin derivatives, whose ability to form adducts with to 2-amino ethyl diphenyl boric acid (Naturstoff reagent) is routinely exploited to visualize flavonoids in fluorescence microscopy (Agati et al., 2009). Thus, ACNs complexed to B, and the subsequent reduction of free B in the leaf, was hypothesized to be responsible for the greater tolerance of purple-leafed sweet basils to B excess when compared to other acyanic cultivars (Landi et al., 2013; Landi et al., 2014; Pardossi et al., 2015).

Beyond the role of these complexes in aboveground plant tissue, ACN-Me^{n+} complexes were also studied in roots (Fedenko, 2006a, 2007, 2008; Fedenko et al., 2008; Hale et al., 2001, 2002; Shemet and Fedenko, 2005), where (obviously) they cannot serve a photo-protective role, but rather they might preserve plant aboveground portion from excessive Me^{n+} uptake. The evidence of ACN-Me^{n+} creation in maize roots was confirmed for Pb, Cd, Fe, Mo, Mg, Al, Ni and V (Fedenko, 2006a, 2007, 2008; Shemet and Fedenko, 2005). An in-depth investigation of ACN-Pb^{2+} formation in maize roots revealed that ACN-Pb^{2+} binding was reversible, pH-dependent (Fedenko, 2006a), and Cy-3-glu-Pb^{2+} formation occurred in a Pb^{2+}-dose-dependent manner (Fedenko, 2007). Noteworthy, it was also reported that pre-incubation of *Allium cepa* roots in ACN-rich extracts lowered the mitotic disturbance and abnormality (c-metaphases, sticky and lagging chromosomes, chromosome bridges, binucleate cells, micronuclei, "budding" nuclei and nucleoli partly outside nuclei) induced

by heavy metal toxicity (Cd, Pb, or Cr) in meristematic cell of *A. cepa* roots, thus suggesting further protective mechanism(s) attributable to ACN-Me^{n+} (Glińska et al., 2007).

Despite the aforementioned evidences which suggest that ACNs may alleviate metal/metalloid toxicity by sequestration of supernumerary ions into ACN-Me^{n+}, only few works have tested this possibility. Confirmation of this role would confer an additional ecological meaning to this class of pigments, whose versatility has probably represented the key of their evolutionary success in plants.

3. Spectrophotometric criteria for *in vitro* detection of anthocyanin-metal complexes

Proposed spectral parameters for *in vitro* identification of ACN-Me^{n+} binding can be classified according to the following analytical techniques: (i) UV-vis absorption spectra and colorimetry techniques for optical transmission; (ii) difference absorption spectra; (iii) solid-phase detection of ACN-Me^{n+}. The first two techniques involve the determination of spectral parameters in solutions, whereas the third assesses reflectance spectra and colorimetry parameters of isolated Me^{n+}-containing ACN preparations/products in solid phase. Various aspects of the aforementioned techniques are detailed below.

3.1. UV-vis absorption spectra and colorimetry techniques for optical transmission

The structure of ACN includes fully delocalized π-conjugated system. Binding to Me^{n+} decreases the energy needed to cause light-induced electron transition in this chromophore system. Thus, the most distinctive indicators of ACN-Me^{n+} formation are the shift of maximum absorption (λ_{max}) toward longer wavelengths of visible region (bathochromic shift) and increase in the intensity of maximal absorbance intensity (ΔA_{max}, so called hyperchromic effect), which are accompanied by changes of color solution. To date, a great number of the studies have investigated those spectral markers (e.g. Sigurdson and Giusti, 2014; Sigurdson et al., 2016; Trouillas et al., 2016). The goals of those studies vary greatly, so it is worthy to classify them according to different aspects:

Qualitative and quantitative determination, kinetic and thermodynamic studies: Studies of ACNs and Al^{3+} interactions were mostly comprehensive as compared to other metals. For example, Al^{3+} ions are used as a shift reagent for the qualitative identification of the ACNs bearing B ring catechol or pyrogallol moieties (Fossen and Andersen, 2006) and a spectrophotometric method for quantitative ACN determination in edible plant sources was developed (Bernal et al., 2015). Moreover, the methodical approach using thermodynamic and kinetic studies was proposed for the investigation of the chemical network formed by ACNs with Al^{3+} and Ga^{3+} ions (Brouillard et al., 2010; Dangles et al., 1994; Elhabiri et al., 1997; Moncada et al., 2003). This approach enables the study of the color shifts from reddish to bluish, based on the ACN complexation with both Me^{n+}.

Besides the abovementioned examples, kinetic and thermodynamic parameters of ACN-Me^{n+} binding were studied for other metals, including Cu^{2+} (Smyk et al., 2008). This reaction involves two stages: ACN-Cu^{2+} complexation ('fast' stage), and reduction of Cu^{2+} and oxidation of ACN in the formed metallocomplex ('slow' stage).

Effect of different metal ions on anthocyanin-metal complexes formation: Comparative studies of ACN complexation with different Me^{n+} have confirmed the universal nature of this reaction and evidenced differences on the formation of ACN-Me^{n+} on the base of the specific atomic structure of each Me^{n+}. Sigurdson et al. (2016) investigated the chelation of five Me^{n+} (Mg^{2+}, Al^{3+}, Cr^{3+}, Fe^{3+}, Ga^{3+}) with Cy and acylated Cy-derivatives (from red cabbage, chokeberry) at different pH (3-8) and with different ACN:Me^{n+} ratios. Bathochromic shifts and hyperchromic effects were the common manifestations of ACN-Me^{n+} interaction occurring at different values of pH; in that experiment the greatest bathochromic shifts was found at pH 6, whereas the most prominent hyperchromic effect was obtained at pH 5. Bathocromic shift was minimal for divalent Mg^{2+}, whereas bathochromic shifts for ACN-Me^{n+} were maximal for trivalent Me^{n+} (which are more electron rich) and decreased in the following row: $Fe^{3+} \approx Ga^{3+} > Al^{3+} > Cr^{3+}$. Greater stability of trivalent than divalent ions was confirmed by the higher Me^{n+}-binding energies of Cy-Al^{3+} *versus* Cy-Mg^{2+} complexes (Esteves et al., 2011).

~~In view of the evidence~~, that Me^{n+} binds principally to the quinoidal base, which dominates at the increased pH values (6-8) in the equilibrium of different ACN forms (Fig. 3) (Trouillas et al., 2016), we concentrated our effort to study the chelation effect of different Me^{n+} at pH 7 (Fedenko, 2006a, 2006b; Fedenko et al., 2005). In detail, the complexation of 18 different Me^{n+} (Cs^{+}, Mg^{2+}, Ca^{2+}, Mn^{2+}, Fe^{2+}, Co^{2+}, Ni^{2+}, Cu^{2+}, Zn^{2+}, Sr^{2+}, Cd^{2+}, Ba^{2+}, Pb^{2+}, Al^{3+}, Cr^{3+}) and three metal-containing anions (VO_3^{-}, MoO_4^{2-}, WO_4^{2-}) with Cy-3-glu (extracted from maize roots) were studied. Values of λ_{max} of Cy-3-glu complexed with different Me^{n+} was bathochromically shifted compared to its flavylium form and the value of that shift ($\Delta\lambda_{max}$) ranged from 10 to 66 nm. However, it is important to note that Me^{n+} bind to the quinoidal base and not to the flavylium ion (see above). Thus, unlike abovementioned researches, the bathochromic shift should be calculated using λ_{max} of quinoidal base rather than that of flavylium ion. In our experiments, $\Delta\lambda_{max}$ ranged from 38 to 14 nm. These considerations should be taken into account for further improve the analytical value of the techniques used to detect the ACN-Me^{n+} binding.

Reproduction of blue petals absorption spectra: Identification of bathochromic shift has also been used to study blue-purple flower absorption spectra and the main results could be separated in two aspects: (i) non-stoichiometric ACN metallocomplexes, and (ii) metalloanthocyanins. Non-stoichiometric ACN metallocomplexes had been identified in blue petals of various species (see

section 2). In *H. macrophylla*, the bathochromic shift was observed during the interaction of Dp-derivatives with Al^{3+} (Schreiber et al., 2010, 2011) and under the presence of the copigments in the reproduction solutions (Kondo et al., 2005; Yoshida et al., 2008). For *T. gesneriana*, the model system consisting of Dp-derivatives and copigments (flavanol glycosides and Fe^{3+}) (Momonoi et al., 2012; Shoji et al., 2007) was used. The 'reconstruction' of the blue color of *Phacelia campanula* petals was performed by mixing Dp-derivative with Al^{3+} or Fe^{3+} (Mori et al., 2006). The blue pigment found in *Meconopsis grandis* petals was modeled by mixing Cy-derivative compounds, flavanols, $Fe^{3+}$and Mg^{2+} ions (Yoshida et al., 2006).

Mori et al. (2008) performed reconstruction experiments to confirm that metalloanthocyanins are stoichiometric, self-assembled, metal-complex pigments consisting of six molecules of ACNs, six molecules of flavones and two Me^{n+}. Visible absorption spectra of the reproduction solution (Dp-derivatives, apigenin and Mg^{2+}) appeared to be closely related to the native cyanosalvianin isolated from petals of *S. uliginosa* (Mori et al., 2008). Similarly, the structure of nemophilin isolated from *N. manziesii* petals was confirmed by the mix of Pt-derivatives, apigenin, Mg^{2+} and Fe^{3+} ions (Yoshida et al., 2015). In the structure of nemophilin, Mn^{2+} can be replaced by Zn^{2+}, Mg^{2+}, Cd^{2+}, whereas Fe^{3+} by Al^{3+}, Ga^{3+}, In^{3+}, ~~this~~ resulting ~~in~~ a creation of metalloanthocyanin-like complexes (Yoshida et al., 2015).

Color modification and stabilization of anthocyanins as colorants: ACN-Me^{n+} interaction is widely exploited for some industrial applications, such as to change ACN color from red to blue, and stabilize ACN-based colorants (Cavalcanti et al., 2011; Somaatmadja et al., 2006). For example, chelation of Al^{3+} and Fe^{3+} with Cy- and Dp- derivatives isolated from different plant species (eggplant, red raspberry, red cabbage, black currant, black carrot, chokeberry) cause intense violet and blue colors (Sigurdson and Giusti, 2014). In some cases, additional ingredients are used to ~~stabilize~~ a complexes, such as pectins (Buchweitz et al., 2012, 2013b), polysaccharide- and gelatin-based gels (Buchweitz et al., 2013a). When sugar beet pectin and isolated pectin fractions were used as stabilizers for ACN-Fe^{3+} and ACN-Al^{3+} complexes, their stability decreased in the row: Dp-3-glu > Cy-3-glu > Pt-3-glu independently to the use of Fe^{3+} or Al^{3+} (Buchweitz et al., 2012). To monitor the complexation, instead of bathochromic shift determination, the investigators used their own criterion: the area under the absorption curve in the range of 580-700 nm, corresponding to the blue tones (Buchweitz et al., 2012). During the *in vitro* interaction of ACNs (from bilberry fruits) with Al^{3+} and flavocommelin, a blue complex pigment was obtained, which was the analogous of natural commelinin (Asada and Tanmura, 2012).

In some other cases ACNs are used as textile dye and the Me^{n+}-chelation feature of ACNs is studied in model systems to maximize the use of Me^{n+} as mordant (Vankar and Bajbai, 2010; Vankar and Shukla, 2011; Wang et al., 2014). In addition, bathochromic shift was found when λ_{max}

for TiO_2 nano-crystalline films sensitized with Mv-3-fructoside was compared to that of Mv-3-fructoside *per se* (Gokilamani et al., 2014), the effect used to maximize light absorption and production of naturally dye-sensitized TiO_2-based solar cell.

Chromogenic reagent for the spectrophotometric quantification of trace metals: The capacity of ACNs to bind different Me^{n+} is also exploited as an eco-friendly approach for the quantification of trace metals in biological and environmental samples (Ekere et al., 2014; Okoye et al., 2012, 2013; Ukwueze et al., 2009). Cy-derivatives isolated from flowers of *Hibiscus* and blackberry fruits were utilized as a sensitive metallochromic indicator in view of the ability to detect changes of UV-vis absorption parameters as a result of their interaction with a plethora of Me^{n+}. The bathochromic shift in ~~vis~~ wavelengths was registered for Cy complexed with Pb (II), Cr (III) and Cd (II) at different pH in methanol and ethanol solutions (Ukwueze et al., 2009). Batochromic ~~shift was~~ also observed for the complexes of Cy with Zn (II), Co (II), Cr (III), Cu (II), Fe (II) in mixed aqueous solutions at pH 5 (Okoye et al., 2012). When Cy complexed with Pb (II), As (III), Cd (II), Hg (II), Ni (II) in mixed aqueous solutions, bathochromic shift (74.6-117.8 nm) was more prominent than that occurring in ~~vis~~ waveband (3.6-8.4 nm) (Okoye et al., 2013). However, when Cy reacted with Bi (II), Sn (II), Mn (II), V (III), Se (II) in mixed aqueous solutions, the opposite tendency was observed in relation to the direction of λ_{max} shift in UV region (5-20 nm hypsochromic shifts) (Ekere et al., 2014).

Counteracting metal toxicity in plants: ~~In view of~~ the incremented absorbance of ACN-Me^{n+} (as compared to the ACN moiety *per se*) in both the UV and the visible ~~region of solar spectrum~~ (Everest et al., 1921; Kondo et al., 1992; Schreiber et al., 2010; Yoshida et al., 2009) it is presumable that ACN-Me^{n+} might offer a further line of defence against excess of harmful irradiance, especially when chloroplast functioning is already impaired by metal toxicity (detailed in section 2). In addition, sequestration of toxic Me^{n+} in peripheral cell layers or their exclusion from cytosolic space (i.e. due to apoplast accumulation and vacuolar storage) are mechanisms commonly adopted by plant to concentrate Me^{n+} in plant tissues where they are less harmful (Hale et al., 2002) and perhaps it is not just a case that both metal ions and ACNs accumulate in the same site in plants experiencing Me^{n+} toxicity. Those include not only photosynthetic tissue but also plant roots (Fedenko, 2007, 2008; Fedenko et al., 2008; Shemet and Fedenko, 2005), which would prevent plant to uptake supernumerary Me^{n+} (see section 2).

Even though less exploited than the hyperchromic effect and bathochromic shift, changes of color parameters could be considered as additional markers of ACN-Me^{n+} in solution. These optical characteristics could be determined based on the transmittance of the light passing through colored solutions with the use, for example, of *CIE* $L^*a^*b^*$ color model which is based upon color-opponent

theory (Trouillas et al., 2016). Generally, the bluing effect that occurs in solution due to the ACN-Me^{n+} formation is accompanied by the decrease in the lightness (L^*) and in values of color coefficient (b^*) whereas values of hue angle (H^*), saturation (C^*) and total color difference (ΔE^*) usually increase (Trouillas et al., 2016). Color parameters were used for the detection of ACNs binding in solution with Al^{3+} (Sigurdson and Giusti, 2014), Cd^{2+} (Fedenko et al., 2005a), Sn^{2+} (Wang et al., 2014), K^+ (Czibylya et al., 2012). However, colorimetric parameters were prevalently utilized for identification of ACN-Me^{n+} in intact plant tissues or for solid-phase investigations as detailed below (see sections 3.3 and 4).

3.2. Difference absorption spectra

In the majority of studies of ACN-Me^{n+} involving UV-vis absorption spectroscopy, the chelation effect is predominately described in terms of bathochromic shift and hyperchromic effect (Sigurdson and Giusti, 2014; Sigurdson et al., 2016). However, in some cases changes in visible λ_{max} could be only slightly perceivable because of high background absorbance, thus other type of analyses over the spectra could be much more informative, such as difference spectroscopy (Sigurdson et al., 2016). A difference spectrum is the difference between two absorption spectra (such as ACN *versus* ACN-Me^{n+} ones) and can be obtained (i) mathematically by subtraction of one absolute spectrum from another or (ii) by placing one compound in the reference cell and the other in the test cuvette. The use of such methodical approach is demonstrated in Fig. 4, exemplified by the interaction between Cy-3-glu and Pb^{2+} in solution (Fedenko, 2006a). At pH = 0.9 the flavylium form of the Cy-3-glu dominates (λ_{max} = 530 nm), whereas increment of pH up to 7 leads to the prevalent formation of the quinoidal base (λ_{max} = 582 nm) (Fig. 4, curve 1). Presence of Pb^{2+} in the solution at pH = 7 results in its complexation, causing a bathochromic shift to 599 nm, and hyperchromic effect (Fig. 4, curve 2). Registering the difference absorption spectra of Cy-3-glu-Pb^{2+} solution *versus* Cy-3-glu solution (pH 7) enables obtaining the difference spectral curve 3 (Fig. 4) having two λ_{max} at 440 and 631 nm and a λ_{min} at 540 nm. The second λ_{max} (631 nm) is associated with the bathochromic shift of the vis band of the Cy-3-glu-Pb^{2+} complex, whereas the hyperchromic effect was recorded for both λ_{max} (440 and 631).

This technique was used to investigate the interactions of Cy-3-glu with 18 metal ions (Fedenko, 2006a, 2006b; Fedenko et al., 2005). ~~Resulted difference spectra~~ differed in the number of λ_{max} and λ_{min} depending on the type of the Me^{n+}. The presence of three groups sharing similar directions in the changes of the spectral parameters enabled us to discriminate three groups of Me^{n+}. The first group was characterized by the presence of a long-wavelength maximum (649 and 607 nm) and λ_{min} (605 and 534 nm) for Fe^{2+} and VO_3^-, respectively. The second group of Me^{n+} (Cs^+, Mn^{2+}, Sr^{2+}, Cd^{2+}, Ba^{2+}, Mg^{2+}, Cu^{2+}, Pb^{2+}, WO_4^{2-}) showed two λ_{max}, differing in their related

intensity (440-475, 605-673 nm) and two λ_{min} (475-596 nm). The third group (Ca^{2+}, Co^{2+}, Ni^{2+}, Zn^{2+}, Al^{3+}, Cr^{3+}, MoO_4^{2-}) had the most evident fine structure of their difference spectra expressing three λ_{max} (437-470, 515-555, 631-675 nm) and two λ_{min} (480-495 and 555-626 nm).

The comparison between absolute and difference absorption spectroscopy techniques for the identification of the ACN-Me^{n+} chelation effects leads to the following conclusions: First of all, the presence of long-wavelength maximum in 605-675 nm range, causing the color evolution of ACN-Me^{n+} complexes (bathochromic shifts of 23-93 nm for this maximum compared to the unassociated Cy-3-glu at pH 7), is the common feature of the difference absorption spectra for all studied Me^{n+}. However, the use of conventional absorption spectroscopy revealed difference of λ_{max} to occur only for five Me^{n+} (Mg^{2+}, Co^{2+}, Cu^{2+}, Pb^{2+}, MoO_4^{2-}), ranging in 4-17 nm, whereas hypsochromic shifts were detected for all the other Me^{n+}. Thus, shifts of λ_{max} detected by difference absorption spectroscopy are a more generalized manifestation of the chelation with respect to the use of conventional absorption spectroscopy. Secondly, registering the 'pure' spectral differences between the unassociated quinoidal base and the metallochelate allows detecting the specific effect each Me^{n+} using the specific pattern of λ_{max} and λ_{min} in the difference spectrum. In contrast to very finely structured difference spectra, the conventional absorption spectra could demonstrate only qualitative band widening, possibly caused by the superposition of several closely-positioned λ_{max}. Thirdly, hyperchromic effect could be detected at each λ_{max} in difference spectrum separately. In contrast to this, the maximum in conventional absorption spectra could demonstrate hypsochromic effect due to the band broadening. For these reasons, the difference spectroscopy could be in most cases much more informative as compared to the conventional visible absorption spectroscopy for the detection of the ACN-Me^{n+}.

It should be noted that another pH-differential method is used in some studies, such as the determination of the total monomeric ACN content (Giusti and Wrolstad, 2001). That method is based on the structural changes of ACN chromophore accompanying the pH-dependent changes between pH 1.0 (colored flavylium form) and 4.5 (colorless hemiketal form) and includes determination of the differences in the absorbance at λ_{max} of 520 nm. In contrast to this methodical approach (Giusti and Wrolstad, 2001), our analytical technique (Fedenko, 2006a, 2006b; Fedenko et al., 2005a) enables registration of the dependence between ΔA_{max} and the wavelength [$\Delta A_{max} = f(\lambda)$] to estimate the effect of Me^{n+} upon the ACN chromophore in specific binding conditions (pH, ACN:Me^{n+} ratio etc.).

3.3. Solid-phase identification of anthocyanin-metal complexes

Yet another variant for the *in vitro* identification of ACN-Me^{n+} consists in the determination of spectral characteristics of ACN-Me^{n+} obtained after their precipitation/inclusion in solid or

semisolid matrixes, such as precipitation of ACN-Me^{n+} upon the addition of Me^{n+} to ACN-rich extracts or chemosorption of ACNs on metal-containing matrixes. The following features of the solid-phase detection of ACN-Me^{n+} binding should be noted. First, the structure of the metallocomplex is fixed in solid state and the dynamic equilibrium of various structural forms, which are possible in solution, is absent. Second, it is possible to identify the associated chromophore in conditions of incomplete binding of the ACN moiety with Me^{n+} when non-stoichiometric complexes are created. Solid-phase *in vitro* investigation is the closest analogue of ACN-Me^{n+} detection in intact plant tissues and they share similar analytical techniques, i.e. reflectance spectroscopy and color measurement.

To overcome the problem related to the high optical density of ACN-Me^{n+}, it is possible to determine their reflectance parameters after homogenization with MgO powder (Fedenko et al., 2005a). This operation decreases the reflectance intensity of ACN-Me^{n+} given that MgO (which represents the standard for white color in reflectance spectroscopy) fully reflects visible light without any effect on the position of λ_{max} in reflectance spectrum of the investigated specimens. Reflectance spectroscopy allows the quantitative determination of Me^{n+} as well as identification of the ACN chromophore, which is modified due to the binding with Me^{n+}, using the position of λ_{max} in visible reflection spectra. Analogous to the measurements in solution, the use of absorption units instead of transmittance units to record the reflectance spectra enables the detection of ACN-Me^{n+} bathochromic shift (when compared to λ_{max} of ACN *per se*). As an example, Fedenko et al. (2005b) found that λ_{max} was 564 nm in the reflectance spectrum of the precipitated Dp-Mg^{2+}-Fe^{2+} metallocomplexes (isolated from blue flowers of *Lupinus polyphyllus* Lindl.). Analogous λ_{max} value was detected for Dp-Pb^{2+} complexes derived by the precipitation of pigment extracted from this plant species (Fedenko et al., 2005b). For complexes of Cy-3-glu (isolated from maize roots) with Ca^{2+}, Fe^{2+}, Cu^{2+}, Al^{3+}, Cr^{2+}, Cd^{2+} and Pb^{2+} values of λ_{max} in reflectance spectrum ranged from 540-605 nm and bathochromic shifts in the range of 105 nm were registered after complexes formation at pH = 0.9 (Fedenko, 2006a, 2006b; Fedenko et al., 2005a). In case of competitive binding of Cy-3-glu with Cd^{2+} and Pb^{2+} with further precipitation of the metallocomplex, the position of λ_{max} in the reflectance spectrum of this metallocomplex (586 nm) did not coincided with the position of λ_{max} for the Cy-3-glu-Pb^{2+} (605 nm) or Cy-3-glu-Cd^{2+} (597 nm) complexes (Fedenko et al., 2005b).

Reflectance characteristics of ACN-Me^{n+} in solid phase could be transformed into color parameters with the use of different color models. In the XYZ color system, the value of dominating wavelength (λ_d) in the region of blue wavebands could be the diagnostic marker of the chelation. Thus, for Cy-3-glu-Pb^{2+} complexes (mixed in MgO powder) λ_d value of 482 nm was registered (Fedenko, 2006a). Blue coloration of ACN-Fe^{3+} chelates in different gel matrixes was confirmed by the parameters of *CIE* $L^*a^*b^*$ color system (Buchweitz et al., 2013a). The same color system was

used for the estimation of the effect of Sn^{2+} (as a mordant) on the stability of ACN extracts isolated from *Liriope platyphylla* fruit for dyeing of silk (Wang et al., 2014).

3.4. Summarizing the general criteria for the detection of the binding between anthocyanins and metals and metalloids

Before concluding about the diagnostic importance of *in vitro* ACN-Me^{n+} binding criteria and before the next section about the *in vivo* detection of ACN-Me^{n+}, the factors affecting chelation of ACN-Me^{n+} in solution should be highlighted and summarized.

Anthocyanin structure: Stable ACN-Me^{n+} are preferentially created by ACNs with catechol or pyrogallol moieties in the B ring (Cy, Dp, Pt). Creation of stable ACN-Me^{n+} is less probable for ACNs with a single hydroxy-substitute in the B ring given that the resulting complexes are generally unstable. However, such complexes could be created under certain conditions (Gokilamani et al., 2014, Zaffino et al., 2015).

pH of the solution: Chelation effect is most efficient for the anionic quinoidal base which dominates at pH 6-8 (Fig. 3). Creation of ACN-Me^{n+} at pH < 6 could be explained by the fact that the presence of Me^{n+} leads to the shift of dynamic equilibrium toward the creation of more reactive intermediates which are eliminated from the reaction medium due to the binding with the Me^{n+}. It should be noted that colorless catechol-Me^{n+} complexes could be produced in certain conditions (Buchweitz, 2016) and metallocomplexes which does not absorb the visible light were produced in mixed aqueous solutions at pH 5 for different Me^{n+} (Ekere et al., 2014).

Anthocyanin:metal ratio: Excess of Me^{n+} over the concentration of ACN molecules induces higher rate of ACN-Me^{n+} formation and larger bathochromic shift and hyperchromic effect, especially out of optimal region for complexes formation (pH 6-8) where Me^{n+} and ACN binding is usually less efficient (Sigurdson et al., 2016). In our opinion, such a tendency could be explained by the fact that the creation of reactive anionic quinoidal base increases when pH increases up to 6-8, thus less quantities of Me^{n+} are needed to shift the dynamic equilibrium (Fig. 3).

Reaction medium: ACN-Me^{n+} binding can take place in aqueous solutions, alcohols, mixed aqueous solutions. Metallocomplexes can also be produced by chemosorption of ACN onto different solid/semisolid matrices.

Metal (metalloid) structure: ACN complexes with 28 Me^{n+} or metal oxides were produced: three monovalent (K, Cs, Ag), 14 bivalent (Mg, Sn, Cu, Ca, Mn, Fe, Co, Ni, Sr, Cd, Ba, Pb, Hg, Zn), and 7 trivalent (Al, Ga, Fe, Cr, Bi, V, In) cations; and three anions (MoO_4^{2-}, VO_3^-,WO_4^{2-}) and

a metal oxide (TiO_2). The ability of ACNs to bind to metalloids, i.e. Se (II) and As (III) had also been confirmed. For B, the process of complex formation between ACN and borate was proposed to occur during pigment separation obtained by electrophoretic techniques (Bednar et al., 2003). These results allow us to state that the ability to bind metals and metalloids is a general feature of ACN, even though the probability of ACN-Me^{n+} formation is strictly dependent on the reactive capability of every single metal/metalloid as well as the stability of resulting complexes. Bearing in mind the factors affecting formation of ACN-Me^{n+}, the relations between spectrophotometric indexes (characteristics, indicators) should be analyzed in terms of *in vitro* detection of ACN-Me^{n+} binding.

Batochromic shift: The shift of λ_{max} toward longer wavelengths is the common sign of more conjugated chromophore system that could result from the binding (or association) of ACN moiety with other compounds, such as Me^{n+}. During the determination of $\Delta\lambda_{max}$ of ACN-Me^{n+} it is of crucial importance which ACN form is used as the reference. As a general rule, $\Delta\lambda_{max}$ during ACN-Me^{n+} binding is determined in visible region ($\Delta\lambda_{max}^{vis}$) against flavylium or quinoidal form ACN form. However, in some cases $\Delta\lambda_{max}^{vis} \leq 0$, which could indicate the absence of the binding effect or the superposition of unassociated and chelated ACN forms in the solution. Taking into consideration that ACNs have additional absorption band in the UV region, it is possible to determine the $\Delta\lambda_{max}^{uv}$ against this band of ACN flavylium form. For a specific Me^{n+}, $\Delta\lambda_{max}^{uv}$ could be greater than $\Delta\lambda_{max}^{vis}$ (Okoye et al., 2013). The area under the absorption curve in the 500-700 nm region could be used as another criterion of the bluing effect resulting from ACN-Me^{n+} binding (Buchweitz et al., 2013b). The presence of long-wavelength maximum in differential spectrum could be more informative for the detection of bathochromic shift, as this approach enables to detect 'pure' spectral difference between the samples under comparison (Fedenko, 2006a, 2006b; Fedenko et al., 2005a). When spectra of ACN-Me^{n+} are compared to those of their relative quinoidal base, obtained differences reflect the direct effect of the Me^{n+} binding upon the chromophore system of ACN. If metallocomplex is created with colorless hemiketal or chalcone forms of ACN, $\Delta\lambda_{max}^{uv}$ should be preferentially used as the discriminative criterion. Bathochromic shift can also be detected by λ_{max} in visible region of the reflectance spectrum of ACN-Me^{n+} complex in solid state against its unassociated flavylium form in solution (Fedenko, 2006a, 2006b Fedenko et al., 2005a).

Hyperchromic effect: Increase in A_{max} could be another criterion for the detection of more conjugated chromophore system as a result of ACN-Me^{n+} binding. In some cases, $\Delta A_{max} < 0$; this effect could be due to the band broadening resulting from the superposition of un-associated and chelated ACN forms. Registering the difference spectra allows detecting positive ΔA_{max} values in each maximum (Fedenko, 2006a, 2006b; Fedenko et al., 2005a). It should be noted that bathochromic shift and hyperchromic effect are common markers for both ACN-Me^{n+} binding and

ACN copigmentation, which can take place due to the association with other compounds, with or without participation of Me^{n+} (Trouillas et al., 2016).

Band broadening: This phenomenon interferes with the detection of the ACN-Me^{n+} complexes due to the overlapping of chromophores bands with adjacently positioned λ_{max}^{vis}. In such cases the determination of $\Delta\lambda_{max}^{vis}$ and ΔA_{max} during ACN-Me^{n+} binding through difference spectroscopy can be much more informative than parameters of absolute spectra (Fedenko, 2006a, 2006b; Fedenko et al., 2005a).

Chromatic criteria: Spectral distribution of the intensity of optical radiation after the interaction of light beam with ACN-Me^{n+} (optical transmittance in case of solutions, or reflectance in case of solid state) can be transformed into appropriate color parameters, in accordance with the physical theory of color vision (Ohta and Robertson, 2006). In *CIE* $L^*a^*b^*$ color model, the bluing effect due to ACN-Me^{n+} is accompanied by the decrease of L^* (lightness) and b^* coefficient, the increase of saturation (C^*) and hue angle (h^*), as well as the increase in total color difference (ΔE^*) compared to the ACN flavylium form (Trouillas et al., 2016). On the other hand, the value of λ_d in blue colors region is a key marker of ACN-Me^{n+} complexes formation by using the *CIE XYZ* color model (Fedenko, 2006a).

Thus, ACN-Me^{n+} can be detected *in vitro* by the integrated approach which involves different spectrophotometric indicators. The understanding of the relations between those indicators, as well as their diagnostic capabilities, enables their use for more complicated and sophisticated *in vivo* diagnostics of ACN-Me^{n+} binding.

4. Identification of anthocyanin-metal binding *in vivo*

While interaction of ACNs and Me^{n+} ~~could~~ be modeled *in vitro* taking ~~due~~ consideration ~~of~~ various factors ~~(~~pH, ACN:Me^{n+} ratio, stabilizing components, etc.~~)~~, direct identification of the chelation effects in plant tissues is complicated due to the following reasons:

- the probability of ACN-Me^{n+} formation is determined by a certain number of factors: uptake of the Me^{n+} by the plant, specificity and amount of Me^{n+} accumulations, species-specific ACN biosynthesis, ACN transport and accumulation, competitive binding to other endogenous chelators (glutathione, metallothioneins, phytochelatins, carboxylic acids, etc.);
- the binding may not occur simultaneously for all ACN molecules which are accumulated in plant tissue; thus different ratios of chelated and unassociated ACN forms is possible;
- the creation of both metalloanthocyanins with defined structure as well as non-stoichiometric ACN-Me^{n+} with unidentified composition is possible;

- different mechanisms of ACN association can result in similar changes in spectrophotometric criteria of ACN chromophore system; copigmentation is one of such alternative mechanisms which can occur both with or without Me^{n+} participation, this causing bathochromic shift/hyperchromic effect in spectral curve independently to Me^{n+} presence;

Taking into consideration the abovementioned issues, the variety of known methods for spectrophotometric *in vivo* investigation of ACN-Me^{n+} binding will be described below concerning i) metalloanthocyanins of blue flowers with confirmed structure; ii) ACNs localized in plant roots which undergo the effects of exogenous supply of Me^{n+}.

4.1. Blue and purple petals

Protocyanin, which is responsible for blue colors of *C. cyanus* flowers is one of the metalloanthocyanins with a well-determined stoichiometric structure (Yoshida et al., 2009). This supramolecular pigment consists of six molecules of acylated Cy, six molecules of acylated apigenin, one Fe^{3+} ion, one Mg^{2+} ion and two Ca^{2+} ions (Takeda, 2006). Fe^{3+} and Mg^{2+} bind to the quinoidal base of ACN moiety, while two Ca^{2+} ions link with flavone moiety (copigments) and stabilize the resulting supramolecular complex (Takeda, 2006). In addition to pure blue coloration, the variation of petal color is a characteristic feature of *C. cyanus* flowers (Fedenko and Struzhko, 2000) and such color variations were quantitatively characterized by using *CIE XYZ* and *CIE* $L^*a^*b^*$ color systems (Fedenko and Struzhko, 2000). According to *CIE XYZ* model, those types of flowers differed in chromaticity coordinates (*x* and *y*) with correspondent differences in the values of λ_d and P_e (Fig. 5, the triangle denotes the range of purple colors). The C1 type had minor amount of flavylium form of Cy; its *x*, *y* coordinates were positioned adjacently to the coordinates of white equal-energy point, with λd in the range of red colors (625 nm). In C5 type, where metallochelate form dominates, the color stimulus matched the blue color (λd = 470 nm). In C2, C3, and C4 types, the *x*, *y* coordinates were in the range of purple colors, which indicates the superposition of unassociated and chelated forms of Cy. The increase in the manifestation of the binding effect in lines C2-C3-C4-C5 was also confirmed by the concurrent decrease of b^* via *CIE* $L^*a^*b^*$ color system. Two separated bands at 575 and 680 nm were found in the reflectance spectrum of C5 flowers (Fig. 6), which correspond to the characteristic bands for protocyanin. In C2 petals, the main λ_{max} was 523 nm in the reflectance spectrum, suggesting the dominance of flavylium form, while the shoulder at 660 nm indicated only minor amounts of chelated form. To achieve better resolution of the maxima on the spectral curve, the first spectral derivative was used, which confirmed the presence of long-wavelength band similarly to the band in C5 type. Gradual increase in the chelated form over unassociated counterpart was also supported by the values of the ratio of

the band intensities in derivative reflectance spectra of those chromophores (Fedenko and Struzhko, 2000). Thus, the use of derivative spectroscopy could be a useful instrument to increase resolution of spectral maxima and to achieve better identification of chelated form when it exists in the presence of unassociated Cy in petals. Experimental data resulted from the use of abovementioned spectral techniques allowed us to explain both the basis for intra-specific color variation in *C. cyanus* flowers during *in vivo* creation of ACN-Me^{n+}, as well as the phenomenon of purple coloration of plant tissues (Fedenko and Struzhko, 2000). According to the physical theory of human color perception (Ohta and Robertson, 2006), the effect of purple color is attributed to mixing of two color stimuli, the first in the range of red colors and the second in the range of blue colors. When localized in outer tissues, red stimulus is caused by flavylium form of ACNs whereas blue stimulus is determined by the presence of metallochelates. Different ratios between those structures when present *in vivo* create their superposition resulting in color variability with different hues of purple petal coloration. Thus, each particular metallochelate of Cy has been found as responsible for the creation of intra-specific polychromism in *C. cyanus* petals (Fedenko and Struzhko, 2000).

Another mechanism for petal color variation in *N. menziesii* was suggested by Yoshida et al. (2015)~~,~~ ~~this attributable to~~ the *in vivo* coexistence of both Mg-Mg nemophilin (metalloanthocyanin with Pt glycoside as ACN chromophore) and Fe-Mg nemophilin. Batochromic shift in visible reflectance spectra of blue or purple petals was used for the detection of *in vivo* binding between Cy-glu and Al^{3+} in *Camellia japonica* (Tanikawa et al., 2016), Dp-glu and Fe^{3+} in *T. gesneriana* (Shoji et al., 2007), Dp-glu and Mg^{2+} in *S. uliginosa* (Mori et al., 2008), and Dp-3-glu and Al^{3+} in *Hydrangea* petals (Kodama et al., 2016). Color parameters of *CIE* $L^*a^*b^*$ system were used for the determination of the role of Al^{3+} and Fe^{3+} in color evolution (red-purple-blue) of flower petals (Momoni et al., 2012; Kodama et al., 2016; Tanikawa et al., 2016). Dependence between color parameters and Fe^{2+}, Ca^{2+}, Mg^{2+}, Mn^{2+} content in petals of different varieties of *Gerbera* was also pointed out (Akbari et al., 2013a, 2013b).

Identification of native metalloanthocyanin complexes in blue or purple petals is also possible by comparing λ_{max} in visible absorption spectra with the use of absorption spectroscopy even though this requires the use of plant preparations which can transmit light (pre-evacuated petals, pressured juice, isolated protoplasts) (Kondo et al., 2005; Mori et al., 2006, 2008; Schreiber et al., 2011; Yoshida et al., 2006, 2008, 2015).

4.2. Anthocyanin-metal complexes in roots

In addition to the possible ecological role of ACN-Me^{n+} in flower petals, the formation of ACN-Me^{n+} in other plant tissues/organs might also represent a detoxification mechanism in plants

which experience luxury availability of trace metals (see section 2). ~~In view of~~ the key role exerted by plant root apparatus in relation to the uptake of Me^{n+}, the spectrophotometric criteria of ACN-Me^{n+} binding were investigated in root tissues of maize that was chosen as model plant due to following reasons (Fedenko, 2006a, 2007, 2008; Fedenko et al., 2008; Shemet and Fedenko, 2005): First, maize is considered as a metal excluder, where root barrier prevents Me^{n+} from accumulation in above-ground organs, thus favoring Me^{n+} accumulation in the roots (Aliyu and Adamu, 2014). Second, characteristic feature of maize is the accumulation of Cy-3-glu in various cells and tissues, including cells of root parenchyma (Holton and Cornish, 1995), and this ACN has demonstrated many times *in vitro* ability to bind different Me^{n+} (Fedenko, 2006a, 2008; Fedenko et al., 2005a).

Binding between Cy-3-glu and Me^{n+} was studied using reflectance spectroscopy in roots detached from intact plants (Fedenko, 2006a, 2007, 2008; Fedenko et al., 2008) and batochromic shifts (ranging from 4.9 to 29.7 nm) were registered in ~~vis~~ reflectance spectra when roots were treated with nine metals (Mg^{2+}, Fe^{2+}, Cd^{2+}, Ni^{2+}, Pb^{2+}, Al^{3+}, VO_3^-, MoO_4^{2-}, $Cr_2O_7^{2-}$). The use of difference spectroscopy improved the informativity of ACN-Me^{n+} formation in roots due to a better resolution of the shift of maximum absorption of the chromophore system when modified by the binding with Me^{n+}. Difference reflectance spectra of roots treated with Mg^{2+} *vs* control plants revealed a maximum in 560-660 nm range, while positive value of ΔA_{max} indicated an increase of ACN-Me^{n+} absorption. Band broadening due to ACN-Me^{n+} chelation was also detected using the specific indicator 'form coefficient' (FC). This parameter was calculated from the reflectance spectral in 535-780 nm range (Fedenko, 2008) and its value was found to decrease with the formation of ACN-Me^{n+}. In terms of color measurements, treatment of roots with some Me^{n+} led to decreased values of P_e and color coefficients L^*, a^* and b^* and, on the other side, increased values of ΔE^* when compared to intact roots (Fedenko, 2008). When Pb^{2+} was used to test its effect on the formation of complexes with Cy-3-glu in maize roots (Fedenko, 2007), a dose-dependent increase of the *in vivo* creation of Cy-3-glu–Pb^{2+} complexes was found, as supported by the significant coefficients arising from the regression between color parameters of the roots (P_e, L^*, a^*, b^* and ΔE^*) *versus* Pb^{2+} concentration.

Spectrophotometric parameters revealed the reversible nature of Cy-3-glu–Pb^{2+} binding in maize roots in model experiment with sequential treatments of root tissue with Pb^{2+} ions, HCl (which induces Cy-3-glu–Pb^{2+} disruption) and Pb^{2+} ions again (Fedenko, 2006a). Treatment of naturally-pigmented root sections with Pb^{2+} ions resulted in the creation of Cy-3-glu–Pb^{2+} complexes as confirmed by the bathochromic shift (of 14.6 nm) in reflectance spectrum, by the presence of maximum at 640 nm in difference spectrum, and by color coordinates of resulted color laying within purple color range (Fig. 7). Subsequent treatment of root segments with HCl led to breakdown of the complexes with recovery of flavylium ACN form, causing hypsochromic shift

toward 530 nm in reflectance spectrum (compared to Cy-3-glu–Pb^{2+} containing roots) with dominating wavelength in the range of red colors (Fig. 7). Third treatment of those roots with Pb^{2+} ions led again to the formation of Cy-3-glu–Pb^{2+} complexes, with return of color coordinates to the region of purple colors, as the result of superposition of two color stimuli: associated (red) and un-associated (blue) forms of the pigment (Fig. 7).

When maize seedlings were grown with various concentrations of Cd^{2+}, it was found that increased ACN accumulation in roots is accompanied by *in vivo* chelation of ACN with Cd^{2+} ions (Shemet and Fedenko, 2005). This effect was supported by the bathochromic shift registered in reflectance spectra of roots excised from seedlings grown under Cd^{2+} exposure when compared to the roots grown in water.

4.3. Interrelationships among spectrophotometric criteria

Spectrophotometric criteria used for the detection of ACN-Me^{n+} in plant tissues are schematized in Fig. 8. The scheme consists of four blocks: 1) colorimetry of plant tissues; 2) visible reflectance spectroscopy of plant tissues; 3) visible absorption spectra of plant preparations with native metallocomplexes; 4) spectrophotometric criteria for the reproduction of ACN-Me^{n+} binding in model systems. Those blocks are arranged according to the informative value of corresponding method.

At first stage of the investigation colorimetry of plant tissues, based on both *CIE XYZ* and *CIE* $L^*a^*b^*$, should be used to be able to benefit from advantages of both models (Fig. 8, block 1). Differently to *CIE* $L^*a^*b^*$, the *CIE XYZ* system is more related to the physical parameters of color rather to than to the color features as perceived by the human eye given that its parameters (*X, Y, Z*) are directly calculated from the spectral distribution of light energy. Transformation of *X, Y, Z* into chromaticity coordinates (*x, y*) enables to locate the color of plant specimen onto the color gamut (Fig. 5, 7) and to calculate dominating wavelength λ_d and excitation purity P_e. Main diagnostic advantage of these parameters (*x, y,* λ_d, and P_e) lies in the fact that they allow *in vivo* identification of either unassociated ACN or chelated ACN-Me^{n+}, as well as their simultaneous presence (Fedenko, 2006a; Fedenko and Struzhko, 2000). *CIE* $L^*a^*b^*$ color model system uniformly covers the entire spectral range of visible by human eye, thus enabling calculation of color differences. For this reason it is recommended for industrial applications (Sant'Anna et al., 2013). *CIE* $L^*a^*b^*$ parameters (L^* a^* b^*, h^*, C^*, ΔE^*) are usually utilized for the detection of ACN-Me^{n+} in flower petals (Momoi et al., 2012; Kodama et al., 2016; Tanikawa et al., 2016).

The second block of spectrophotometric criteria (Fig. 8) includes different indicators measured by ~~vis~~ reflectance spectroscopy in intact plant tissue. Notably, when reflectance spectrum is expressed in terms of absorbance units, the position of λ_{max} can indicate the localization of ACNs in

outer plant tissues either in metal-associated or unassociated form. When λ_{max} cannot be detected due to spectral band broadening (as a result of mixing different forms of the pigment), the calculation of FC in the region of expected λ_{max} can be more efficient. In a case of coexistence of unassociated and ACN-Me^{n+} forms the use of both the following techniques is the most informative approach. The first technique involves obtaining the first and second derivatives of reflectance spectrum, which increases the resolution of both bands and their detection by the location of respective maximums λ'_{max} and intensities A'_{max}. In the second technique, the difference spectrum is calculated, using two intact plant specimens: one containing ACN-Me^{n+} complexes and another containing unassociated ACNs. In this case, the location and intensities of the maxima and minima (λ_{max}, ΔA, λ_{min}) in difference spectrum should be considered as the markers of 'pure' spectral changes between the both forms of ACN.

Position of λ_{max} in visible absorption spectra of plant preparation containing native ACN-Me^{n+} (pre-evacuated petals, pressured juice, isolated colored protoplasts) could be an additional criterion for detecting ACN-Me^{n+} complexation (block 3), whereas in contrast to the block 3, the preparation of pigment extracts according to block 4 is performed in acidic medium, leading to the destruction of native metallocomplexes. Interactions between flavylium form of ACN and Me^{n+} could be reproduced *in vitro* in model systems using a toolset of spectrophotometric criteria, as summarized in chapter 4 of present review.

Thus, the proposed aggregate of spectrophotometric criteria for ACN-Me^{n+} interactions involves the detection of ACN-Me^{n+} binding both *in vitro* and *in vivo*. It should be noted, that the practical value of specific spectrophotometric indicators depends on the intensity of chelation effect which occurs *in vivo*. Thus, the first step on the identification of ACN-chelation effect should comprise the calculation of chromaticity coordinates (*x*, *y*) followed by calculations of λ_d and P_e. When ACNs are the only pigment class presents in plant tissue, chromaticity coordinates (*x*, *y*) can reveal three color ranges: 1) blue; 2) red; 3) purple (Fig. 5 and 7) (Fedenko, 2006a; Fedenko and Struzhko, 2000). The variant 1) means that chelated ACN form dominates *in vivo* and, additionally, 'bluish effect' could be supported by the b^*, h^*, C^* parameters and bathochromic shift in visible reflectance spectra of plant tissues. The variant 2) indicates the dominance of red flavylium form of ACN in concomitance with the presence of minor amounts of chelated pigment still capable to modify chromaticity coordinates and to shift the coloration toward the region of purple colors. The variant 3) is the most common case of purple coloration in plant kingdom, which is defined by superposition of two color stimuli – red (flavylium form) and blue (metallocomplexes). In this case, the bathochromic shift in reflectance spectra and *CIE* $L^*a^*b^*$ parameters may not definitely support the binding of ACN and Me^{n+}. This is the reason to use more informative diagnostic criteria, such as FC of the spectral curve as well as parameters of derivative and difference spectra.

5. Conclusions

In this review, we summarize the use of UV-vis spectroscopy techniques for detecting both the *in vitro* and *in vivo* formation of ACN-Me^{n+} in plant tissues. The main purpose is to popularize these techniques to a wide range of plant scientists and to promote the research on the topic, given that the ecological meaning of ACN-Me^{n+} still is a hot topic for plant biologists and ecologists. Many intriguing questions are yet to be answered such as "How do pollinators respond to the changes of petal color when plants experience a condition of metal toxicity and which in turn affects plant fitness?", "Is the role of ACN-Me^{n+} in roots restricted to that of a 'metal barrier' for the aboveground plant tissues?", "In addition to metals, which metalloids can form complexes with ACNs?" Beyond the well-supported ecological meanings of ACNs, a deeper understanding of the roles of ACN-Me^{n+}, when located in different plant tissues (flowers, leaves, roots), would strengthen the versatility of this class of pigments, feature that probably represents their evolutionary success in *Angiospermae*.

References

Agati, G., Stefano, G., Biricolti, S., Tattini, M., 2009. Mesophyll distribution of antioxidant flavonoids in *Ligustrum vulgare* leaves under contrasting sunlight irradiance. Ann. Bot. 104, 853-861.

Akbari, R., Hatamzadeh, A., Sariri, R., Bakhshi, D., 2013a. Analysis of petal pH and metal ions to investigate the mechanism of colour development in Gerbera hybrid. Aust J Crop Sci. 7, 941-947.

Akbari, R., Hatamzadeh, A., Sariri, R., Bakhshi, D., 2013b. Relationship of flower color parameters and metal ions of petal tissue in fully opened flowers of gerbera. J. Plant Stud. 2, 89-96.

Aliyu, H.G., Adamu, H.M., 2014. The potential of maize as phytoremediation tool of heavy metals. Eur. Sci. J. 10, 30-36.

Andersen, Ø.M., Jordhein, M., 2006. The Anthocyanin, in: Andersen, Ø.M. and K.P. Markham (Eds.), Flavonoids: Chemistry, Biochemistry and Applications, CRC Press, Boca Raton, FL, pp. 451-471.

Archetti, M., Doring, T.F., Hagen, S.B., Hughes, N.M., Leather, S.R., Lee, D.W., Lev-Yadun, S., Manetas, Y., Ougham, H.J., Schaberg, P.G., Thomas, H., 2009. Unravelling the evolution of autumn colours: an interdisciplinary approach. Trends Ecol. Evol. 24, 166-173.

Asad, S. A., Muhammad, S., Farooq, M., Afzal, A., Broadley, M., Young, S., West, H., 2015. Anthocyanin production in the hyperaccumulator plant *Noccaea caerulescens* in response to herbivory and zinc stress. Acta Physiol. Plant. 37, 1715.

Asada, T., Tamura, H., 2012. Isolation of bilberry anthocyanidin 3-glycosides bearing *ortho*-dihydroxyl groups on the B ring by forming an aluminum complex and their antioxidant activity. J. Agric. Food Chem. 60, 10634-10640.

Baldisserotto, C., Ferroni, L., Zanzi, C., Marchesini, R., Pagnoni, A., Pancaldi, S., 2010. Morpho-physiological and biochemical responses in the floating lamina of *Trapa natans* exposed to molybdenum. Protoplasma 240, 83-97.

Bauer, V.E., 1958. Phänomenologische theorie der kristallabscheidung an oberflächen. II. Z. Kristallogr. 110, 395-431.

Bednar, P., Tomassi, A.V., Presutti, C., Pavlikova, M., Lemr, K., Fanali, S., 2003. Separation of structurally related anthocyanins by MEKC. Chromatographia 58, 283-287.

Bernal, F.A., Orduz-Diaz, L.L., Coy-Barrera, E., 2015. Exploitation of the complexation reaction of *ortho*-dihydroxylated anthocyanins with aluminum (III) for their quantitative spectrophotometric determination in edible sources. Food Chem. 185, 84-89.

Brouillard, R., Chassaing, S., Isorez, G., Kueny-Stotz, M., Figueiredo, P., 2010. The visible flavonoids or anthocyanins: from research to applications, in: Santos-Buelga C., Escribano-Bailon M. T., Lattanzio V. (Eds.), Recent Advances in Polyphenol Research, Volume 2, Wiley-Blackwell, Oxford, UK, pp. 1-22.

Brown, P.H., Bellaloui, N., Wimmer, M.A., Bassil, E.S., Ruiz, J., Hu, H., Pfeffer, H., Dannel, F., Römheld, V., 2002. Boron in plant biology. Plant Biol. 4, 205-223.

Buchweitz, M., 2016. Natural solutions for blue colors in food, in: Carle, R., Schweiggert, R.M. (Eds.), Handbook on Natural Pigments in Food and Beverages: Industrial Applications for Improving Food Color, Woodhead Publishing, pp. 355-384.

Buchweitz, M., Brauch, J., Carle, R., Kammerer, D.R., 2013a. Application of ferric anthocyanin chelates as natural blue food colorants in polysaccharide and gelatin based gels. Food Res. Int. 51, 274-282.

Buchweitz, M., Brauch, J., Carle, R., Kammerer, D.R., 2013b. Colour and stability assessment of blue ferric anthocyanin chelates in liquid pectin-stabilised model systems. Food Chem. 138, 2026-2035.

Buchweitz, M., Carle, R., Kammerer, D.R., 2012. Bathochromic and stabilising effects of sugar beet pectin and an isolated pectic fraction on anthocyanins exhibiting pyrogallol and catechol moieties. Food Chem. 135, 3010-3019.

Cavalcanti, R.N., Santos, D.T., Meireles, M.A.A., 2011. Non-thermal stabilization mechanisms of anthocyanins in model and food systems-An overview. Food Res. Int. 44, 499-509.

Cervilla, L. M., Blasco, B., Rios, J. J., Rosales, M. A., et al., 2012. Parameters symptomatic for boron toxicity in leaves of tomato plants. J. Bot. Article ID 726206, 17 pp. DOI: 10.1155/2012/726206.

Chalker-Scott, L., 1999. Environmental significance of anthocyanins in plants stress response. Photochem. Photobiol. 70, 1-9.

Cheynier, V., Comte, G., Davies, K. M., Lattanzio, V., Martens, S., 2013. Plant phenolics: recent advances on their biosynthesis, genetics, and ecophysiology. Plant Physiol. Biochem. 72, 1-20.

Czibulya, Z., Horváth, I., Kollár, L., Kunsági-Máté, S., 2012. Unexpected effect of potassium ions on the copigmentation in red wines. Food Res. Int. 45, 272-276.

Dai, L.P., Dong, X.J., Ma, H.H., 2012a. Antioxidative and chelating properties of anthocyanins in *Azolla imbricata* induced by cadmium. Pol. J. Environ. Stud. 21, 837-844.

Dangles, O., Elhabiri, M., Brouillard, R., 1994. Kinetic and thermodynamic investigation of the aluminium–anthocyanin complexation in aqueous solution. J. Chem. Soc. Perkin Trans. 2, 2587-2596.

Doustaly, F., Combes, F., Fiévet, J. B., Berthet, S., Hugouvieux, V., Bastien, O., Vavasseur, A., 2014. Uranium perturbs signalling and iron uptake response in *Arabidopsis thaliana* roots. Metallomics 6, 809-821.

Ekere, N.R., Okoye, C.O.B., Ihedioha, J.N., 2014. Novel simultaneous spectrophotometric determinations of Bi (III), Sn (II), Mn (II), V (III) and Se (II) ions in mixedaqueous solutions. J. Chem. Pharm. Res. 6, 5-8.

Elhabiri, M., Figueiredo, P., Toki, K., Saito, N., Brouillard, R., 1997. Anthocyanin-aluminium and -gallium complexes in aqueous solution. J. Chem. Soc. Perkin Trans. 2, 355-362.

Ellestad, G.A., 2006. Structure and chiroptical properties of supramolecular flower pigments. Chirality 18, 134-144.

Eraslan, F., Polat, M., Yildirim, A., Kucukyumuk, Z., 2016. Physiological and nutritional responses of two distinctive quince (*Cydonia oblonga* Mill.) rootstocks to boron toxicity. Pak. J. Bot. 48, 75-80.

Esteves, L., Otero, N., Mosquera, R.A., 2011. Molecular structure of cyanidin metal complexes: Al (III) versus Mg (II). Theor. Chem. Acc. 128, 485-495.

Everest, A.E., Hall, A.J., 1921. Anthocyanins and anthocyanidins: Part IV. Observations on (a) anthocyan colors in flowers and (b) the formation of anthocyans in plants. Proc. R. Soc. B 92, 150-162.

Fedenko, V.S., 2006a. Binding of lead ions with cyanidin in maize seedlings roots. Fiziologiia i biokhimiia kul'turnykh rastenii = Physiol. Biochem. Cultivated Plants 38, 67-74.

Fedenko, V.S., 2006b. Cyanidin complexation with metal ions. Ukr. Biochem. J. 78, 149-153.

Fedenko, V.S., 2007. Dose effect of cyanidin interaction with lead ions in roots of maize seedlings Ukr. Biochem. J. 79, 24-29.

Fedenko, V.S., 2008. Cyanidin as endogenous chelator of metal ions in maize seedling roots. Ukr. Biochem. J. 80, 102-106.

Fedenko, V.S., Shemet, S.A., Struzhko, V.S., 2005a. Complexation of cyanidin with cadmium ions in solution. Ukr. Biochem. J. 77, 104-109.

Fedenko, V.S., Shemet, S.A., Struzhko, V.S., Priymak K.P., 2008. Method to determine bonding metals in plant tissues. Patent of Ukraine UA 85043.

Fedenko, V.S., Struzhko, V.S., 2000. Cyanidin chelation and polychroism of the flowers of the cornflower. Fiziologiia i biokhimiia kul'turnykh rastenii = Physiol. Biochem. Cultivated Plants 32, 266-272.

Fedenko, V.S., Struzhko, V.S., Stetsenko, T.V., 2005b. Method for identifying metallic complex compounds of anthocyanin pigments. Patent of Ukraine UA 4426.

Fossen, T., Andersen, Ø.M., 2006. Spectroscopic techniques applied to flavonoids, in: Andersen, Ø.M., Markham, K.P. (Eds.), Flavonoids: Chemistry, Biochemistry and Applications. CRC Press, Boca Raton, FL, pp. 37-142.

Foster, J.J., Sharkey, C.R., Gaworska, A.V.A., Roberts, N.W., Whitney, H.M., Partridge, J.C., 2014. Bumblebees learn polarization patterns. Curr. Biol. 24, 1415-1420.

Giusti, M.M., Wrolstad, R.E., 2001. Characterization and measurement of anthocyanins by UV-visible spectroscopy. Curr. Prot. Food Anal. Chem. F:F1:F1.2.

Glińska, S., Bartczak, M., Oleksiak, S., Wolska, A., Gabara, B., Posmyk, M., Janas, K., 2007. Effects of anthocyanin-rich extract from red cabbage leaves on meristematic cells of *Allium cepa* L. roots treated with heavy metals. Ecotoxycol. Environ. Saf. 68, 343-350.

Gokilamani, N., Muthukumarasamy, N., Thambidurai, M., Ranjitha, A., Velauthapillai, D., 2014. Grape pigment (malvidin-3-fructoside) as natural sensitizer for dye-sensitized solar cells. Mat. Renew. Sust. Energ. 3, 1-7.

Gould, K.S., 2010. Muriel Wheldale Onslow and the rediscovery of anthocyanin function in plants, in: Santos-Buelga, C., Escribano-Bailon, M.T., Lattanzio, V. (Eds.), Recent Advances in Polyphenol Research. Wiley-Blackwell, West Sussex, UK, pp. 206-224.

Gould, K.S., Davies K.M., Winefield, C., 2009. Anthocyanins: Biosynthesis, Functions, and Applications. Springer, New York.

Grotewold, E., 2006. The genetics and biochemistry of floral pigments. Annu. Rev. Plant Biol., 57, 761-780.

Guidi L., Penella C., Landi M., 2015. Anthocyanins in Mediterranean diet: common and innovative sources, in: Warner, L.H. (Ed.), Handbook of Anthocyanins: Food Sources, Chemical Application and Health Benefit, Nova Publisher, New York, pp. 1-50.

Hale, K.L., McGrath, S.P., Lombi, E., Stack, S.M., Terry, N., Pickering, I.J., George, G.N., Pilon-Smits, E.A.H., 2001. Molybdenum sequestration in *Brassica*: a role for anthocyanins? Plant Physiol. 126, 1391-1402.

Hale, K.L., Tufan, H.A., Pickering, I.J., George, G.N., Terry, N., Pilon, M., Pilon-Smits, E.A.H., 2002. Anthocyanins facilitate tungsten accumulation in *Brassica*. Physiol. Plant. 116, 351-358.

Hawrylak-Nowak, B., 2008. Changes in anthocyanin content as indicator of maize sensitivity to selenium. J. Plant Nutr. 31, 1232-1242.

Hayashi, K., 1957. Fortschritte der anthocyanforschung in Japan mit besonderer Berucksichti gung der papierchromatographischen Methoden. Pharmazie 12, 245-249.

Hayashi, K., Abe, Y., Mitsui, S., 1958. Blue anthocyanins from the flowers of *Commelina,* the crystallization and some properties thereof. Proc. Jpn. Ac. 34, 373-378.

Holton, T. A., Cornish, E.C., 1995. Genetics and biochemistry of anthocyanin biosynthesis. Plant Cell 7, 1071-1083.

Hughes, N.M., 2011. Winter leaf reddening in 'evergreen' species. New Phytol. 190, 573-581.

Jayantakumar, M., Shukla, V.J. 2014. Simultaneous UV–visible spectrophotometric quantitative determination of heavy metal ions using calibration method of proposed anti-hyperglycaemic formulation using cyaniding as a chromogenic reagent. Int. J. Univers. Pharm. Bio Sci. 3, 329-336.

Kelber, A., Thunell, C., Arikawa, K., 2001. Polarisation-dependent colour vision in *Papilio* butterflies. J. Exp. Biol. 204, 2469-2480.

Kirchner, S.M., Döring, T.F., Saucke H., 2005. Evidence for trichromacy in the green peach aphid, *Myzus persicae* (Sulz.)(Hemiptera: Aphididae). J. Insect Physiol. 51, 1255-1260.

Kodama, M., Tanabe, Y., Nakayama, M., 2016. Analyses of coloration-related components in *Hydrangea* sepals causing color variability according to soil conditions. Hort. J. 85, 372-379.

Kondo, T., Oyama, K., Yoshida, K., 2001. Chiral molecular recognition on formation of a metalloanthocyanin: a supramolecular metal complex pigment from blue flowers of *Salvia patens*. Angew. Chem. 40, 894-897.

Kondo, T., Toyama-Kato, Y., Yoshida, K., 2005. Essential structure of co-pigment for blue sepal-color development of *Hydrangea*. Tetrahedron Lett. 46, 6645-6649.

Kondo, T., Ueda, M., Tamura, H., Yoshida, K., Isobe, M., Goto, T., 1994. Composition of protocyanin, a self-assembled supramolecular pigment from the blue cornflower, *Centaurea cyanus*. Angew Chem. Int. Edit. 33, 978-979.

Kondo, T., Yoshida, K., Nakagawa, A., Kawai, T., Tamura, H., Goto, T., 1992. Structural basis of blue-colour development in flower petals from *Commelina communis*. Nature 358, 515-518.

Kösesakal, T., Ünal, M., 2012. Effects of zinc toxicity on seed germination and plant growth in tomato (*Lycopersicon esculentum* Mill.). Frese. Environ. Bull. 21, 315-324.

Landi, M., 2015. Can anthocyanins be part of the metal homeostasis network in plant? Am. J. Agric. Biol. Sci. 10, 170-177.

Landi, M., Guidi, L., Pardossi, A., Tattini, M., Gould, K.S., 2014. Photoprotection by foliar anthocyanins mitigates effects of boron toxicity in sweet basil (*Ocimum basilicum*). Planta 240, 941-953.

Landi, M., Remorini, D., Pardossi, A., Guidi, L., 2013. Sweet basil (*Ocimum basilicum*) with green or purple leaves: which differences occur in photosynthesis under boron toxicity? J. Plant Nutr. Soil Sci. 176, 942-951.

Landi, M., Tattini, M., Gould, K.S., 2015. Multiple functional roles of anthocyanins in plant-environment interactions. Environ. Exp. Bot. 119, 4-17.

Leão, G.A., de Oliveira, J.A., Felipe, R.T.A., Farnese, F.S., Gusman, G.S., 2014. Anthocyanins, thiols, and antioxidant scavenging enzymes are involved in *Lemna gibba* tolerance to arsenic. J. Plant Interact. 9, 143-151.

Manetas, Y., 2006. Why some leaves are anthocyanic and why most anthocyanic leaves are red? Flora 201, 163-177.

Menzies, I.J., Youard, L.W., Lord, J.M., Carpenter, K.L., van Klink, J.W., Perry, N.B., Schaefer, H.M., Gould, K.S., 2016. Leaf colour polymorphisms: a balance between plant defence and photosynthesis. J. Ecol. 104, 104-113.

Miller, R., Owens, S.J., Rørslett, B., 2011. Plants and colour: flowers and pollination. Opt. Laser Techol. 43, 282-294.

Momonoi, K., Tsuji, T., Kazuma, K., Yoshida, K., 2012. Specific expression of the vacuolar iron transporter, TgVit, causes iron accumulation in blue-colored inner bottom segments of various tulip petals. Biosci. Biotechnol. Biochem. 76, 319-325.

Moncada, M.C., Moura, S., Melo, M.J., Roque, A., Lodeiro, C., Pina, F., 2003. Complexation of aluminum (III) by anthocyanins and synthetic flavylium salts: A source for blue and purple color. Inorg. Chim. Acta 356, 51-61.

Mori, M., Kondo, T., Toki, K., Yoshida, K., 2006. Structure of anthocyanin from the blue petals of *Phacelia campanularia* and its blue flower color development. Phytochem. 67, 622-629.

Mori, M., Kondo, T., Yoshida, K. 2008. Cyanosalvianin, a supramolecular blue metalloanthocyanin, from petals of *Salvia uliginosa*. Phytochem. 69, 3151-3158.

Nigel, C.V., Grayer, R.J., 2008. Flavonoids and their glycosides, including anthocyanins. Nat. Prod. Rep. 25, 555-611.

Ohta, N., Robertson, A.R., 2006. Colorimetry: fundamentals and applications. John Wiley & Sons., West Sussex, UK.

Okoye, C.O.B., Chukwuneke, A.M., Ekere, N.R., Ihedioha, J.N., 2013. Simultaneous ultraviolet-visible (UV-vis) spectrophotometric quantitative determination of Pb, Hg, Cd, As and Ni ions in aqueous solutions using cyanidin as a chromogenic reagent. Int. J. Phys. Sci. 8, 98-102.

Okoye, C.O.B., Okon, E.E., Ekere, N.R., Ihedioha, J.N., 2012. Simultaneous UV-VIS spectrophootometric quantitative determinations of cyanidin complexes of Co, Zn, Cr, Cu, and Fe ions in mixed aqueous solutions. Int. J. Chem. Anal. Sci. 3, 1662-1664.

Ougham, H., Thomas, H., Archetti, M., 2008. The adaptive value of leaf colour. New Phytol. 179, 9-13.

Pardossi, A., Romani, M., Carmassi, G., Guidi, L., Landi, M., Incrocci, L., Maggini, R., Puccinelli, M., Vacca, W., Ziliani, M., 2015. Boron accumulation and tolerance in sweet basil (*Ocimum basilicum* L.) with green or purple leaves. Plant Soil 395, 375-389.

Park, W., Han, K.H., Ahn, S.J., 2012. Differences in root-to-shoot Cd and Zn translocation and by HMA3 and 4 could influence chlorophyll and anthocyanin content in Arabidopsis Ws and Col-0 ecotypes under excess metals. Soil Sci. Plant Nutr. 58, 334-348.

Pilon-Smits, E., Pilon, M., 2002. Phytoremediation of metals using transgenic plants. Crit. Rev. Plant Sci. 21, 439-56.

Pina, F., Melo, M.J., Laia, C.A., Parola, A.J., Lima, J.C., 2012. Chemistry and applications of flavylium compounds: a handful of colours. Chem. Soc. Rev. 41, 869-908.

Ribi, W., Warrant, E., Zeil, J., 2011. The organization of honeybee ocelli: regional specializations and rhabdom arrangements. Arthropod Struct. Dev. 40, 509-520.

Rodríguez-Gironés, M.A., Santamaría, L., 2004. Why are so many bird flowers red? PLoS Biol. 2, 306-350.

Růžičková, P., Száková, J., Havlík, J., Tlustoš, P., 2015. The effect of soil risk element contamination level on the element contents in *Ocimum basilicum* L. Arch. Environ. Prot. 41, 47-53.

Sant'Anna, V., Gurak, P.D., Marczak, L.D.F., Tessaro, I.C., 2013. Tracking bioactive compounds with colour changes in foods–A review. Dyes Pig. 98, 601-608.

Schreiber, H.D., Jones, A.H., Lariviere, C.M., Mayhew, K.M., Cain, J.B., 2011. Role of aluminum in red-to-blue color changes in *Hydrangea macrophylla* sepals. BioMetals 24, 1005-1015.

Schreiber, H.D., Swink, A.M., Godsey, T.D., 2010. The chemical mechanism for Al^{3+} complexing with delphinidin: A model for the bluing of hydrangea sepals. J. Inorg. Biochem. 104, 732-739.

Shemet, S.A., Fedenko, V.S., 2005. Accumulation of phenolic compounds in maize seedlings under toxic Cd influence. Physiol. Biochem. Cultivated Plants 37, 505-512.

Shibata, K., Shibata, Y., Kasiwagi, I., 1919. Studies on anthocyanins: colour variation in anthocyanins. J. Am. Chem. Soc. 41, 208-220.

Shiono, M., Matsugaki, N., Takeda, K., 2005. Structure of the blue cornflower pigment. Nature 436, 791.

Shoji, K., Miki, N., Nakajima, N., Momonoi, K., Kato, C., Yoshida, K., 2007. Perianth bottom-specific blue color development in tulip cv. Murasakizuisho requires ferric ions. Plant Cell Physiol. 48, 243-251.

Sigurdson, G.T., Giusti, M.M., 2014. Bathochromic and hyperchromic effects of aluminum salt complexation by anthocyanins from edible sources for blue color development. J. Agric. Food Chem. 62, 6955-6965.

Sigurdson, G.T., Robbins, R.J., Collins, T.M., Giusti, M.M., 2016. Evaluating the role of metal ions in the bathochromic and hyperchromic responses of cyanidin derivatives in acidic and alkaline pH. Food Chem. 208, 26-34.

Smyk, B., Pliszka, B., Drabent, R., 2008. Interaction between cyanidin 3-glucoside and Cu (II) ions. Food Chem. 107, 1616-1622.

Somaatmadja, D., Powers, J.J., Hamdy, M.H., 2006. Anthocyanins. VI. Chelation studies on anthocyanins and other related compounds. J. Food Sci. 29, 655-660.

Takahashi, S., Badger, M.R., 2011. Photoprotection in plants: a new light on photosystem II damage. Trends Plant Sci. 16, 53-60.

Takeda, K., 2006. Blue metal complex pigments involved in blue flower color. Proc. Jpn. Acad. B 82, 142-154.

Takeda, K., Hayashi, K., 1977. Metallo anthocyanins. I. Reconstruction of commelinin from its components, awobanin, flavocommelin and magnesium. Proc. Jpn. Acad. 53, 1-5.

Takeda, K., Kubota, R., Yagioka, C., 1985. Copigments in the blueing of sepal colour of *Hydrangea macrophylla*. Phytochem. 24, 1207-1209.

Takeda, K., Yanagisawa, M., Kifune, T., Kinoshita, T., Timberlake, C.F., 1994. A blue pigment complex in flowers of Salvia patens. Phytochem. 35, 1167-1169.

Tanikawa, N., Inoue, H., Nakayama, M., 2016. Aluminum ions are involved in purple flower coloration in *Camellia japonica* 'Sennen-fujimurasaki'. Hort. J. 85, 331-339.

Toyama-Kato, Y., Yoshida, K., Fujimori, E., Haraguchi, H., Shimizu, Y., Kondo, T., 2003. Analysis of metal elements of *Hydrangea* sepals at various growing stages by ICP-AES. Biochem. Eng. J. 14, 237-241.

Trouillas, P., Sancho-García, J. C., De Freitas, V., Gierschner, J., Otyepka, M., Dangles, O., 2016. Stabilizing and modulating color by copigmentation: insights from theory and experiment. Chem. Rev. 116, 4937-4982.

Ukwueze, N.N., Nwadinigwe, C.A., Okoye, C.O.B., Okoye, F.B.C., 2009. Potentials of 3, 31, 41, 5, 7-pentahydroxyflavylium of *Hibiscus rosa-sinensis* L.(Malvaceae) flowers as ligand in the quantitative determination of Pb, Cd and Cr. Int. J. Phys. Sci. 4, 58-62.

Vankar, P.S., Bajpai, D., 2010. Rose anthocyanins as acid base indicators. Electron. J. Environ. Agric. Food Chem. 9, 875-884.

Vankar, P.S., Shukla, D., 2011. Natural dyeing with anthocyanins from *Hibiscus rosa-sinensis* flowers. J. Appl. Polym. Sci. 122, 3361-3368.

Wang, H., Li, P., Zhou, W., 2014. Dyeing of silk with anthocyanins dyes extract from *Liriope platyphylla* fruits. J. Text. Article ID 587497, 9 pp., DOI: 10.1155/2014/587497.

Wehner, R., 2001. Polarization vision-a uniform sensory capacity? J. Exp. Biol. 204, 2589-2596.

Wernet, M.F., Velez, M.M., Clark, D.A., Baumann-Klausener, F., Brown, J.R., Klovstad, M., Labhart, T., Clandinin, T.R., 2012. Genetic dissection reveals two separate retinal substrates for polarization vision in *Drosophila*. Curr. Biol. 22, 12-20.

Yoshida, K., Ito, D., Shinkai, Y., Kondo, T., 2008. Change of color and components in sepals of chameleon *Hydrangea* during maturation and senescence. Phytochem. 69, 3159-3165.

Yoshida, K., Kitahara, S., Ito, D., Kondo, T., 2006. Ferric ions involved in the flower color development of the Himalayan blue poppy, *Meconopsis grandis*. Phytochem. 67, 992-998.

Yoshida, K., Mihoko, M., Kondo, T., 2009. Blue flower color development by anthocyanins: from chemical structure to cell physiology. Nat. Prod. Rep. 26, 857-964.

Yoshida, K., Tojo, K., Mori, M., Yamashita, K., Kitahara, S., Noda, M., Uchiyama S.U., 2015. Chemical mechanism of petal color development of *Nemophila menziesii* by a metalloanthocyanin, nemophilin. Tetrahedron 71, 9123-9130.

Zaffino, C., Russo, B., Bruni, S., 2015. Surface-enhanced Raman scattering (SERS) study of anthocyanidins. Spectrochim. Acta A Mol. Biomol. Spectrosc. 149, 41-47.

Zhang C., Ma Y., Zhao X., Mu, J., 2009. Influence of copigmentation on stability of anthocyanins from purple potato peel in both liquid state and solid state. J. Agric. Food Chem. 57, 9503-9508.

Figure captions

Fig. 1.
Chemical structure of flavylium ion of 2-phenylpenzopyrilium.

Fig. 2.
Chemical structure of the main anthocyanidins found in plants.

Fig. 3.
Structural transformations of cyanidin-3-glucoside in acidic to neutral solution and the different possibility of metal ion (Me^{n+}) binding (modified from Buchweitz, 2016; Pina et al., 2012; Trouillas et al., 2016).

Fig. 4.
Absorption spectra for cyanidin-3-glucoside (Cy-3-glu) at pH 7 (1), Cy-3-glu + Pb^{2+} (pH 7) (2), difference absorption spectrum of Cy-3-glu + Pb^{2+} (pH 7) *vs*. Cy-3-glu (pH 7) (3) (modified from Fedenko, 2006a).

Fig. 5.
Chromaticity coordinates of *Centaurea cyanus* petals with different pigmentation (C1-C5). Dominant wavelengths for C2, C3 and C4 types of coloration are in the range of complementary colors (modified from Fedenko, Struzhko, 2000).

Fig. 6.
Reflectance spectra **(**A**)** and their first-order derivatives **(**B**)** of the petals of *Centaurea cyanus* flowers with different types of coloration (modified from Fedenko, Struzhko, 2000).

Fig. 7.
Chromaticity coordinates of maize seedling roots subjected to different treatments: intact roots (1); roots treated with 10^{-2} M Pb^{2+} (2); roots treated with 10^{-2} M Pb^{2+} followed by the treatment with 0.1 M HCl (3); roots treated with 10^{-2} M Pb^{2+}, then with 0.1 M HCl and treated again with 10^{-2} M Pb^{2+} (4). Dashed triangle outlines the region of purple colors. The arrows show the sequence of treatments. (Modified from Fedenko, 2006a).

Figure 8. Summary of the main techniques utilized for the detection of anthocyanin-metal complexes (ACN-Me^{n+}) in plants. Abbreviations: ΔA_{max}, variation of maximal absorbance intensity; λ_d, dominating wavelength; λ_{max} maximal absorbance wavelenght; λ'_{max}, first derivative of maximal absorbance wavelength; A_{max}, maximal absorbance intensity; A'_{max}, first derivative of maximal absorbance intensity; FC, form coefficient; P_e, excitation purity.

Figure 1

Click here to download Figure: Figure 1.docx

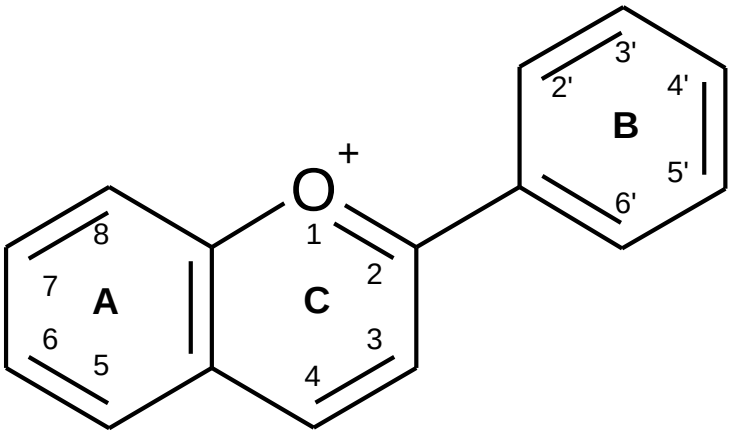

Figure 1.

Figure 2

Click here to download Figure: Figure 2.doc

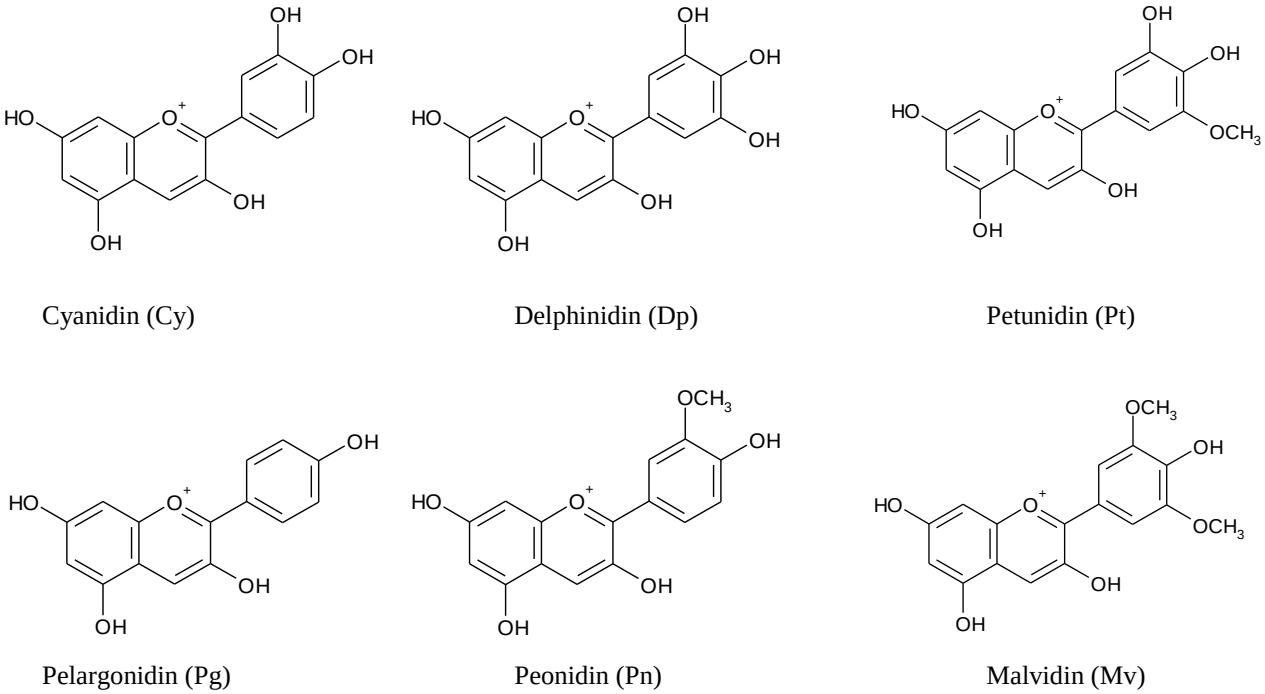

Figure 2.

Figure 3

Click here to download Figure: Figure 3.doc

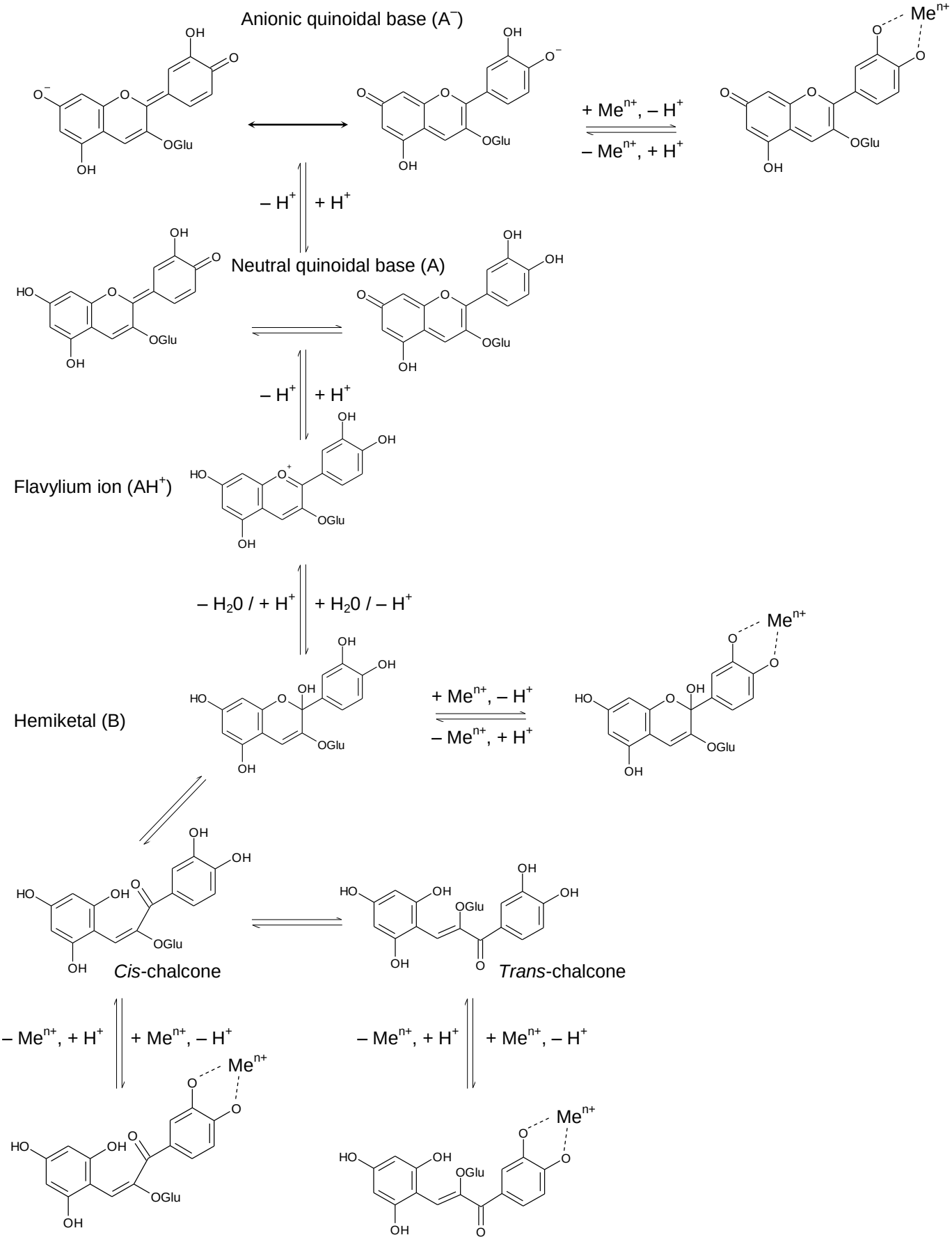

Figure 3.

Figure 4
Click here to download Figure: Figure 4.docx

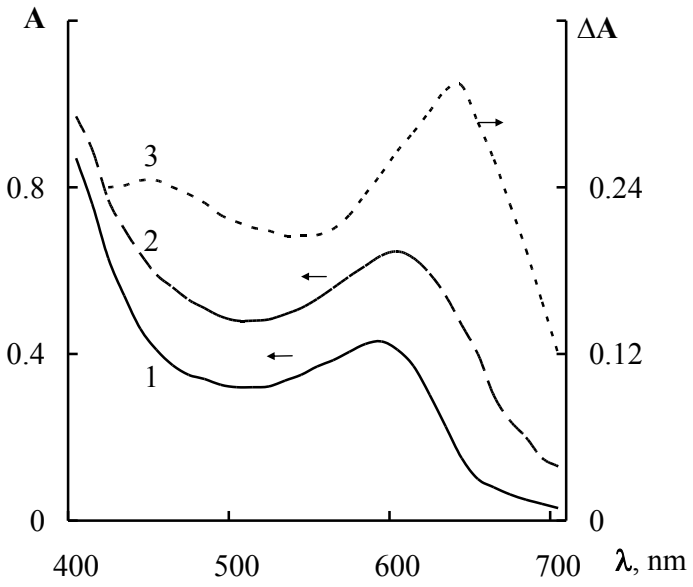

Figure 4.

Figure 5

Click here to download Figure: Figure 5.docx

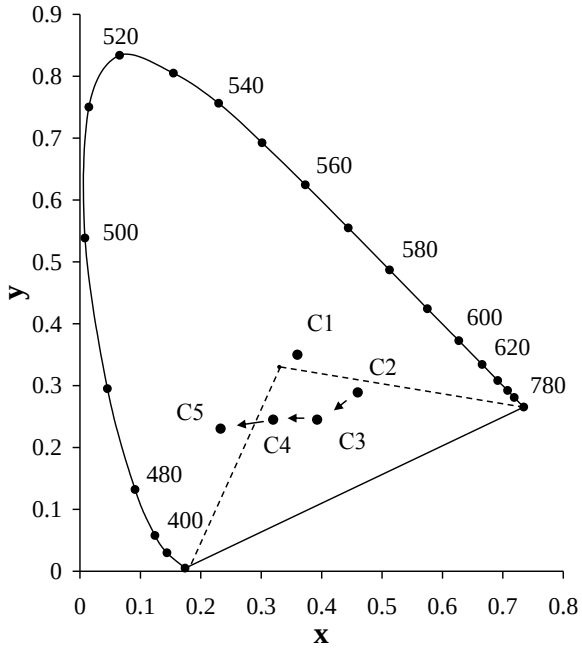

Figure 5.

Figure 6

Click here to download Figure: Figure 6.docx

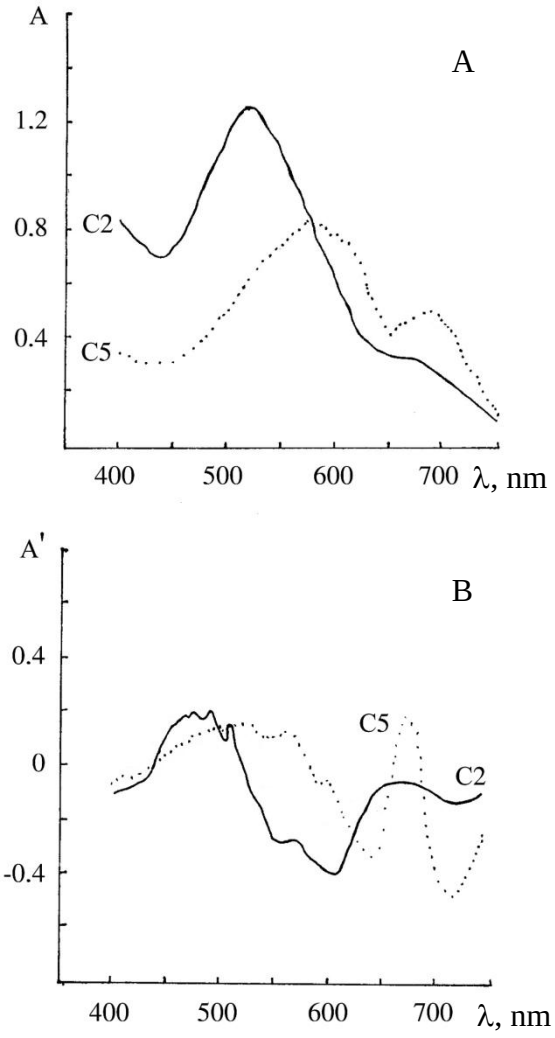

Figure 6.

Figure 7

Click here to download Figure: Figure 7.docx

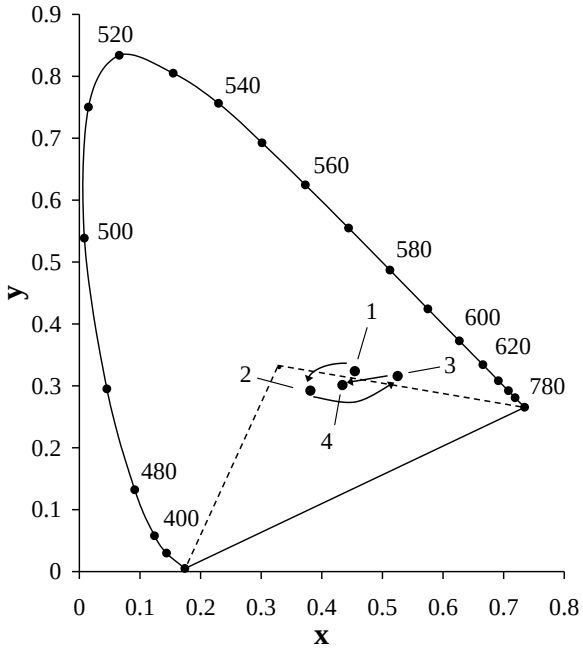

Figure 7.

Figure 8
Click here to download Figure: Figure 8.docx

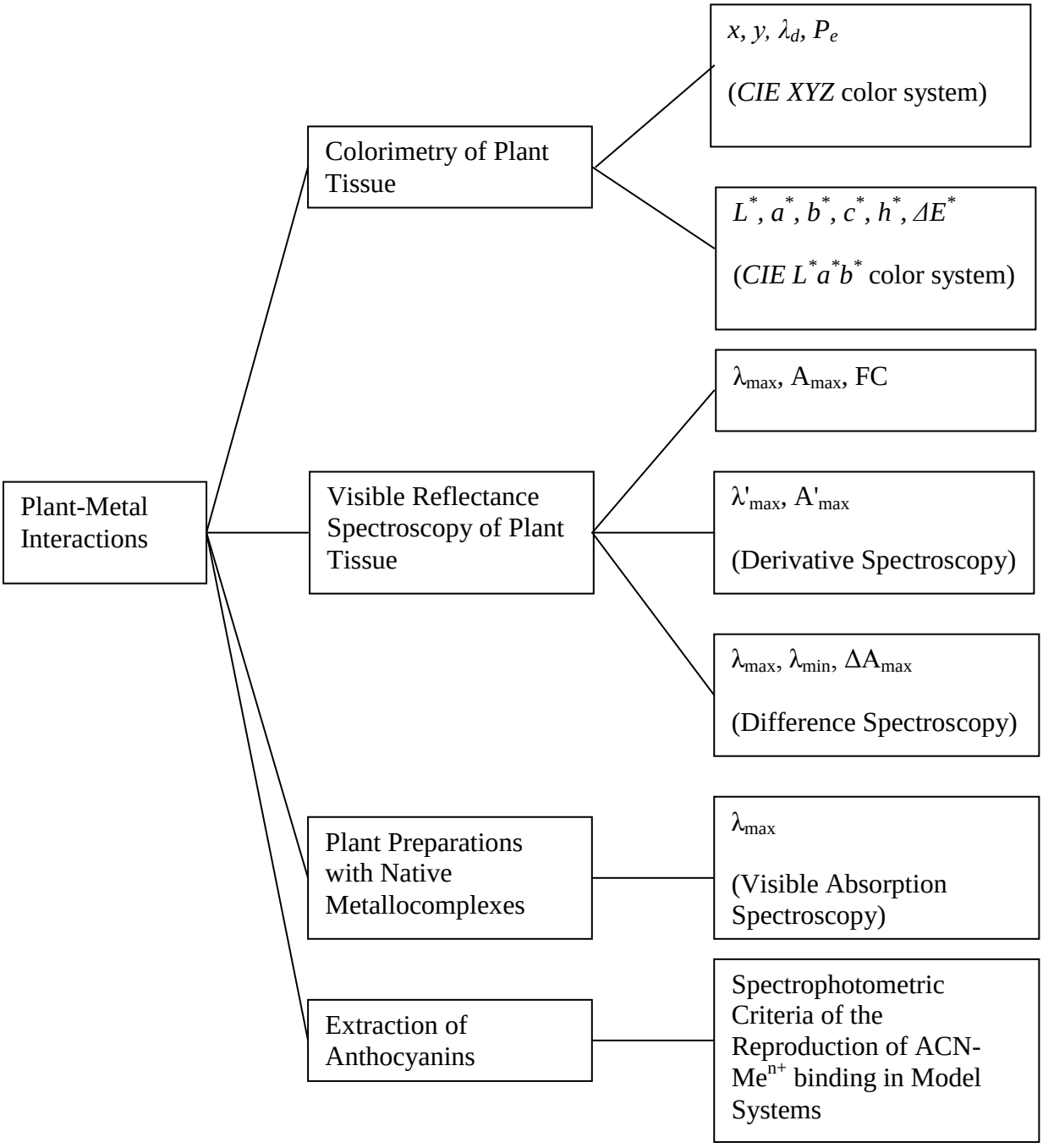

Figure 8.

*Summary

Graphical abstract